



A Rogue's Gallery of V&V Practice

Bill Rider

Computational Shock and Multiphysics Department

Sandia National Laboratories, Albuquerque, NM

wjrider@sandia.gov

July 23, 2010 MeV Summer School Lunch Talk



Quote du jour...

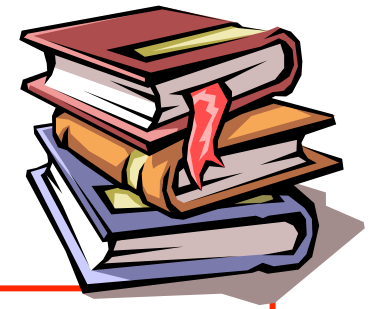
“The purpose of computing is insight, not pictures”–Richard Hamming



© Scott Adams, Inc./Dist. by UFS, Inc.



Some definitions used in V&V



Complementary

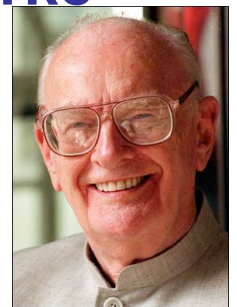
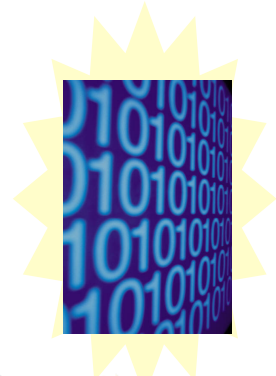
- Verification \approx Solving the equations correctly
 - Mathematics/Computer Science issue
 - Applies to both codes and calculations
- Validation \approx Solving the correct equations
 - Physics/Engineering (i.e., **modeling**) issue
 - Applies to both codes and calculations
- Calibration \approx Adjusting (“tuning”) parameters
 - Parameters chosen for a specific class of problems
- Benchmarking \approx Comparing with other codes
 - “There is no democracy in physics.”*

*L.Alvarez, in D. Greenberg, *The Politics of Pure Science*, U. Chicago Press, 1967.



The nature of the code development is a key aspect to consider.

- How well do the code developers understand what they are working on.
- In some cases the key developers have moved on and are not available...
- ... leading to the “magic” code issue,
 - “Any sufficiently advanced technology is indistinguishable from magic.” Arthur C. Clarke [Clarke's Third Law]
 - Understanding problems can be nearly impossible, or prone to substantial errors,
 - Fixing problems become problematic (bad choices are often made!) as a consequence.



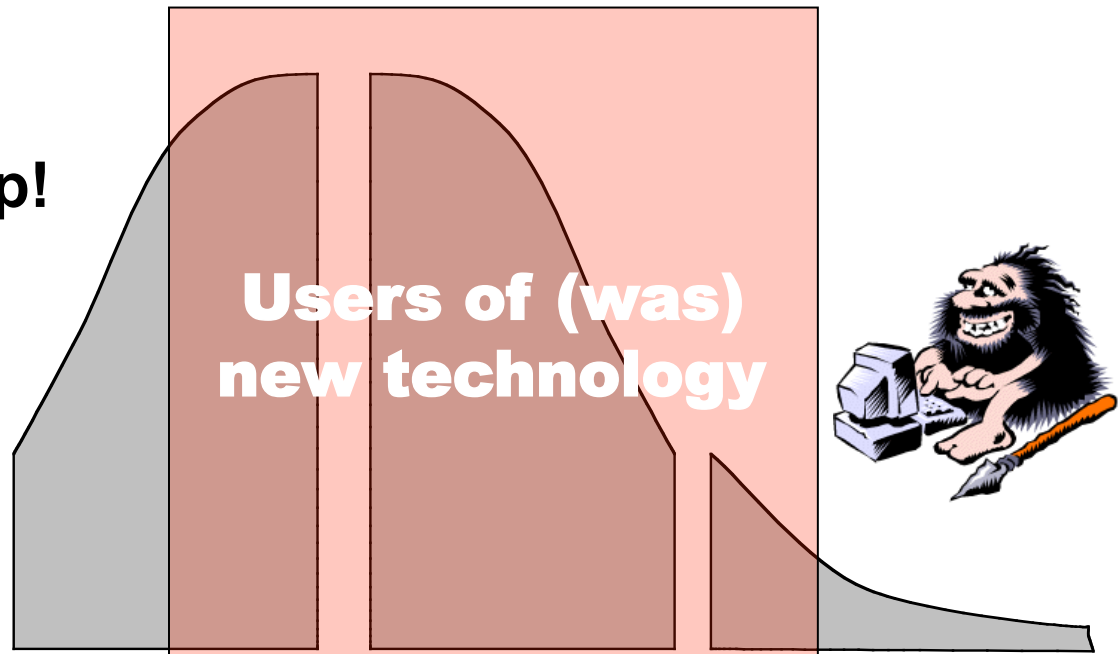
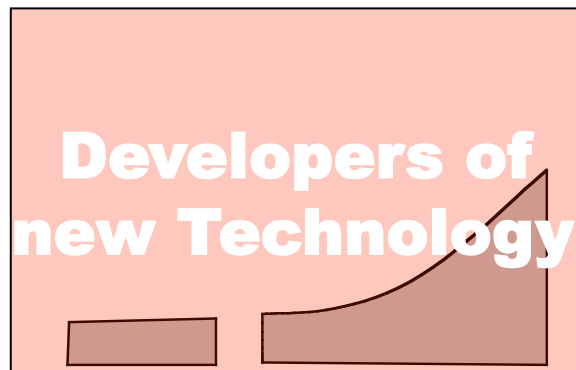
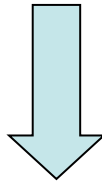


Diffusion of innovation is useful to understand how ideas advance.



“So easy, even a caveman could do it” - Geico

The Gap!



Innovators



Technology Enthusiasts

Early Adopters



Visionaries



Early Majority



Pragmatists

Late Majority



Conservatives

Laggards



Skeptics

Figure adapted from “After the Goal Rush: Creating a True Profession of Software Engineering” by Steve McConnell, Microsoft Press 1999

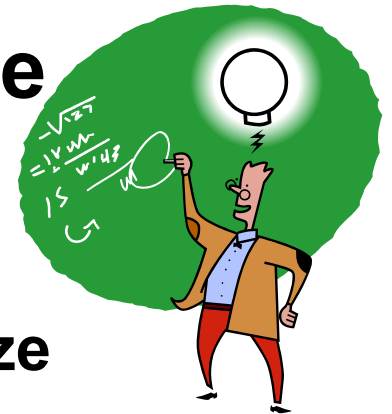


“Most daily activity in science can only be described as tedious and boring, not to mention expensive and frustrating.”

Stephen J. Gould, Science, Jan 14, 2000.



We can see how different the user communities can be.



- If one considers that the journals characterize the leading edge of work in an area.
- **For fluid mechanics, the engineering community has embraced well-defined standards (using V&V)**
- **While the physics community tends to embrace a standard based on expert judgment.**
- These considerations tend to be reflected in practice (*albeit in broad brushes*):
 - Some engineers tend to work to achieve an evidence basis for decisions
 - Most physicists tend to provide their evidence based more strongly on expertise.





I'm going to go through a set of examples next from the literature.

- The examples are taken from the **current (2009 & 2010) literature** for a small subset of journals.
- They **do not** reflect a comprehensive study, the articles were simply chosen from a recent issue of the journal.
- My working thesis is that any issues *are not an indictment of the authors*, but rather a reflection of **accepted practice within the communities** represented by the journals chosen.



Excerpt from the editorial policy of JFE

“Journal of Fluids Engineering disseminates technical information in fluid mechanics of interest to researchers and designers in mechanical engineering. *The majority of papers present original analytical, numerical or experimental results and physical interpretation of lasting scientific value.* Other papers are devoted to the review of recent contributions to a topic, or the description of the methodology and/or the physical significance of an area that has recently matured.”





Excerpt from the editorial policy of JFE (i.e. the fine print)

“Although no standard method for evaluating numerical uncertainty is currently accepted by the CFD community, there are numerous methods and techniques available to the user to accomplish this task. The following is a list of guidelines, enumerating the criteria to be considered for archival publication of computational results in the *Journal of Fluids Engineering*.”

Then 10 different means of achieving this end are discussed, and a seven page article on the topic.



Excerpt from the editorial policy of JFE (digging even deeper, more fine print!)

“An uncertainty analysis of experimental measurements is necessary for the results to be used to their fullest value. Authors submitting papers for publication to this Journal are expected to describe the uncertainties in their experimental measurements and in the results calculated from those measurements and unsteadiness.”

– The numerical treatment of uncertainty follows directly from the need to assess the experimental uncertainty.

- This seems quite reasonable, but as we will see it is uncommon.***



Excerpt from the editorial policy of JFE

“The Journal of Fluids Engineering will not consider any paper reporting the numerical solution of a fluids engineering problem that fails to address the task of systematic truncation error testing and accuracy estimation. Authors should address the following criteria for assessing numerical uncertainty.”

Its difficult to find language this strong for other publications, its also not clear that this policy is uniformly implemented.



Example from JFE

Assessment of Large-Eddy Simulation of Internal Separated Flow

Marco Hahn¹

e-mail: m.hahn@cranfield.ac.uk

Dimitris Drikakis

Department of Aerospace Sciences,
Fluid Mechanics and Computational Science
Group,
Cranfield University,
Bedfordshire MK43 0AL, UK

This paper presents a systematic numerical investigation of different implicit large-eddy simulations (LESs) for massively separated flows. Three numerical schemes, a third-order accurate monotonic upwind scheme for scalar conservation laws (MUSCL) scheme, a fifth-order accurate MUSCL scheme, and a ninth-order accurate weighted essentially non-oscillatory (WENO) method, are tested in the context of separation from a gently curved surface. The case considered here is a simple wall-bounded flow that consists of a channel with a hill-type curvature on the lower wall. The separation and reattachment locations, velocity, and Reynolds stress profiles are presented and compared against solutions from classical LES simulations.

[DOI: 10.1115/1.3130243]

Journal of Fluids Engineering

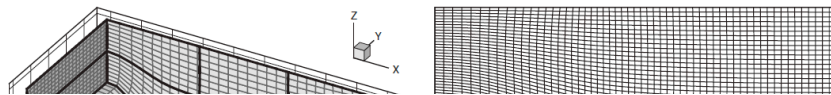
Copyright © 2009 by ASME

JULY 2009, Vol. 131 / 07120

The numerical investigation of high-resolution methods for large-eddy simulation has been carried out using three different computational grids. The computational domain representing the constricted channel extends $9h$ and $4.5h$, and between $2h$ and $3.035h$ in x -, y -, and z -direction, also referred to as streamwise, cross-stream, and vertical directions, respectively. Here, h is the height of the hill-type shape at the lower wall. A H-H-type topology was chosen (Fig. 1(a)) and no-slip boundary conditions are applied at the top and bottom walls of the channel, while periodicity was assumed in the streamwise and cross-stream directions.

Three different grid resolutions have been investigated here: (i) a highly under-resolved grid, referred to as “coarse,” comprising approximately 0.65×10^6 relative uniformly distributed points; (ii) a modified version of the coarse grid with an identical number of points, referred to as “modified,” featuring a finer clustering near the top and bottom walls of the channel; and (iii) a moderately finer grid consisting of 1.03×10^6 points, referred to as “medium,” where the refinement mainly affects the distribution around the hill crest and a slightly better resolution near the bottom wall is achieved; see Figs. 1(b)–1(d). The coarse and medium grids are basically identical to the ones used in previous wall-modeled LES [9]. The characteristic parameters for all three grids, including z^+

choice of
Addition-
simula-



This looks fairly good. Three grids and some degree of quantification. As we'll see its, much more than other papers, but in my opinion not quite enough.

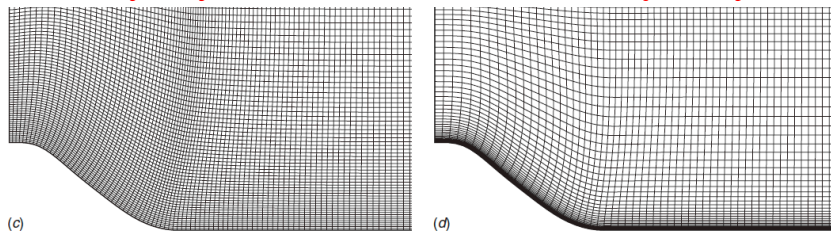
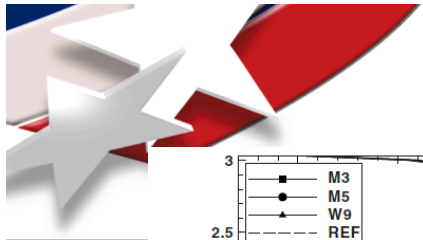


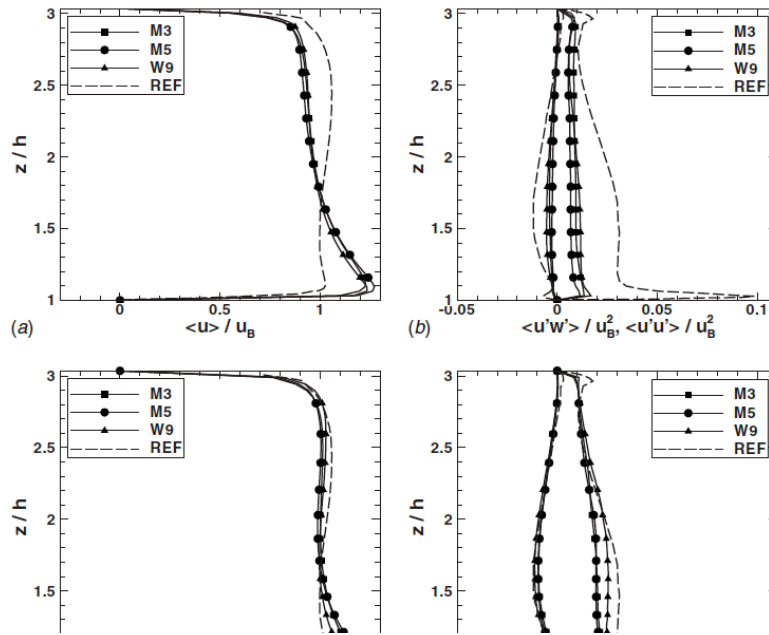
Fig. 1 The computational H-H-type grid topology and the three different grids employed in the simulations of the hill flow

Table 1 Characteristic parameters for the three grids employed here and for the highly resolved reference LES

Grid	$N_x \times N_y \times N_z$	Size	$\Delta x/h$	$\Delta y/h$	$\Delta z/h$	z_{\min}^+	z_{\max}^+
Coarse	$112 \times 91 \times 64$	0.65×10^6	0.08	0.049	0.032	≈ 7	≈ 14
Modified	$112 \times 91 \times 64$	0.65×10^6	0.08	0.049	0.0047	≈ 1	≈ 3
Medium	$176 \times 91 \times 64$	1.03×10^6	0.04	0.049	0.02	≈ 4	≈ 9
Reference	$196 \times 186 \times 128$	4.67×10^6	0.032	0.024	0.0033	≈ 0.5	≈ 1



Example from JFE



No experimental data, and the reference solution has no quantification of its quality its just "highly resolved".

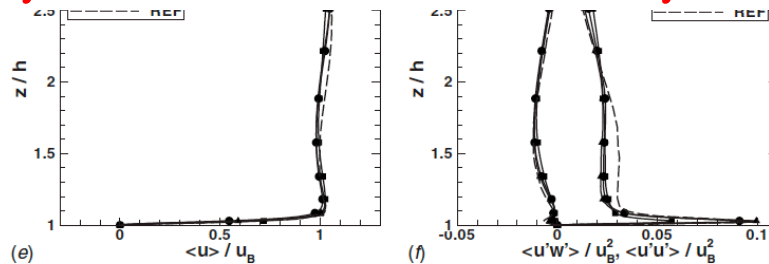


Fig. 3 Comparison of the averaged streamwise velocity and Reynolds stresses near the hill crest at $x/h=0.05$ as obtained by different high-resolution methods on the coarse, medium and modified grids with the reference LES

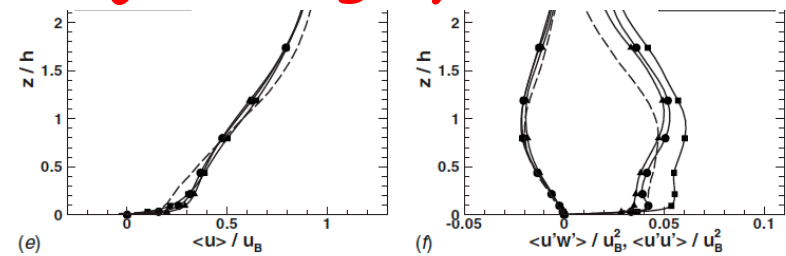
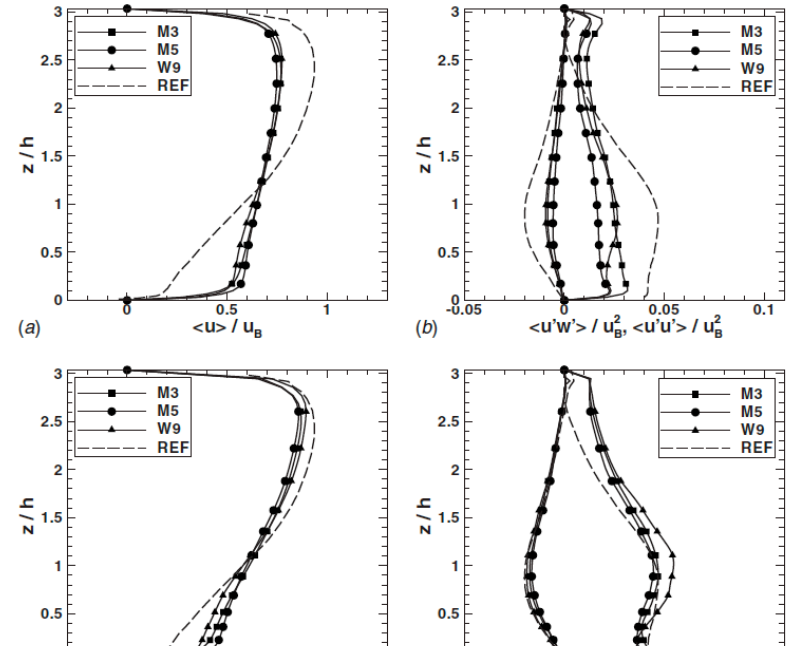


Fig. 5 Comparison of the averaged streamwise velocity and Reynolds stresses after reattachment at $x/h=6$ as obtained by different high-resolution methods on the coarse, medium and modified grids with the reference LES



AIAA Journal has a strong policy.

The AIAA journals will not accept for publication any manuscript reporting (1) numerical solutions of an engineer-

"rules are necessary when people lack judgment".

-John Clifford

AIAA JOURNAL
Vol. 47, No. 8, August 2009

Computational and Experimental Investigation of a Non slender Delta Wing

Raymond E. Gordnier* and Miguel R. Visbal†
**AIAA Research Laboratory, Wright-Patterson Air Force Base, Ohio 45433-7512*

and
Ismet Gursul‡ and Zhijin Wang§
University of Bath, Bath, England BA2 7AY, United Kingdom

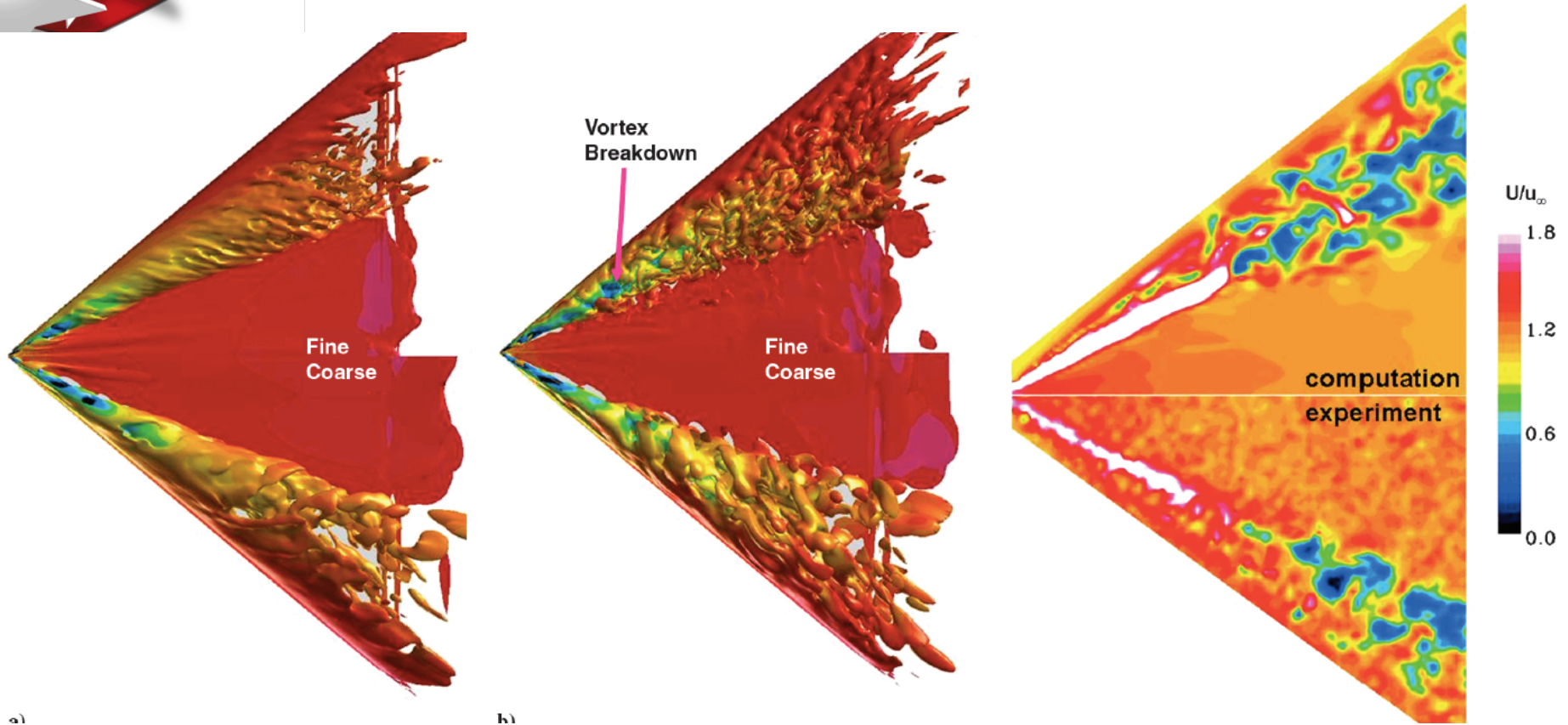
Computational simulations have been performed for a 50-deg-sweep delta wing with a sharp leading edge at a 15 deg angle of attack and moderate Reynolds numbers of $Re = 2 \times 10^5$, $Re = 6.2 \times 10^5$, and $Re = 2 \times 10^6$. A sixth-order compact-difference scheme with an eighth-order low-pass filter is used to solve the Navier–Stokes equations. Turbulence modeling has been accomplished using an implicit large eddy simulation method that exploits the high-order accuracy of the compact-difference scheme and uses the discriminating higher-order filter to regularize the solution. Computations have been performed on a baseline mesh of 11.3×10^6 grid points and a refined mesh of 35×10^6 grid points. An assessment of grid resolution showed that significantly finer-scale features of the flow could be captured on the refined mesh, providing a more accurate representation of the complex, unsteady, separated flow. Comparisons are also made with high-resolution particle image velocimetry images obtained for the two lower Reynolds numbers. The numerical results are examined to provide a description of the mean and instantaneous flow structure over the delta wing, including the separated vortical flow, vortex breakdown, surface flow features, and surface boundary-layer transition near the symmetry plane. The effect of Reynolds number on each of these features is assessed.

The digital particle images from the PIV measurement were taken using an 8-bit charge-coupled device camera with a resolution of 4.2×10^6 pixels. The commercial software package Insight v6.0 and a Hart cross-correlation algorithm were used to analyze the images. In the image processing, an interrogation window size of 32×32 pixels was used to produce the velocity vectors. The effective grid size was varied from 1.5 mm in crossflow planes to 1.8 mm in a plane through the vortex cores. Sequences of 800 and 3000 instantaneous frames, corresponding to the crossflow and vortex core plane measurements, respectively, were taken at a frame rate of 3.75 Hz. The time-averaged velocity and vorticity fields were calculated.

Downstream of breakdown, the fine-grid solution exhibits a much more detailed flow structure with significantly smaller scales being captured, Fig. 6. Both the mean and instantaneous flows on the fine grid show more small-scale features in the outer shear layer that rolls up to form the vortex, Figs. 6a and 6c, as well as in the vortex core itself. Enhanced interactions of these structures with the surface boundary layer are also seen as they move across the wing surface. The resulting turbulent kinetic energy levels are smaller on the fine mesh but the turbulent kinetic energy is more evenly distributed throughout the vortex core. This contrasts with the behavior observed upstream of breakdown.



These figures characterize the results



I cannot find any quantification of error in this paper. Numerical error is never estimated, PIV errors are not estimated.

The strong policy doesn't work if its not followed.



Example from J. Appl. Mech.

Jeong-Hoon Song¹

Postdoctoral Fellow
e-mail: j-song2@northwestern.edu

Ted Belytschko

Walter P. Murphy Professor
McCormick Professor

Theoretical and Applied Mechanics,
Northwestern University,
Evanston, IL 60208-3111

Dynamic Fracture of Shells Subjected to Impulsive Loads

A finite element method for the simulation of dynamic cracks in thin shells and its applications to quasibrittle fracture problem are presented. Discontinuities in the translational and angular velocity fields are introduced to model cracks by the extended finite element method. The proposed method is implemented for the Belytschko–Lin–Tsay shell element, which has high computational efficiency because of its use of a one-point integration scheme. Comparisons with elastoplastic crack propagation experiments involving quasibrittle fracture show that the method is able to reproduce experimental fracture patterns quite well. [DOI: 10.1115/1.3129711]

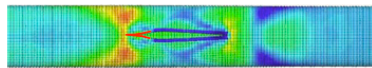
Journal of Applied Mechanics

Copyright © 2009 by ASME

SEPTEMBER 2009, Vol. 76 / 051301-1

For the numerical simulation, we discretized the right segment of the cylinder length of the 91.40 cm with 54,382 four-node quadrilateral shell elements ($h_e \approx 0.90$ mm); see Figs. 8(b) and 8(c). The shell material is aluminum 6061-T6 and we modeled it with J_2 -plasticity, density $\rho = 2780.0$ kg/m³, Young's modulus $E = 69.0$ GPa, Poisson's ratio $\nu = 0.30$, and yield stress $\sigma_y = 275.0$ MPa. We used linear hardening with constant slope $h_p = 640.0$ MPa. The cohesive fracture energy $G_f = 19.0$ kJ/m² is treated in terms of a cohesive law (the assigned fracture energy is based on Refs. [26–28]).

In order to induce unsymmetrical crack propagation with an axisymmetric shell structure and loading, we introduced a small scatter in the yield strength of bulk material. The yield strength at every material point is perturbed by factors ranging from -5.0% to 5.0% : The perturbation factor is obtained from a log-normal



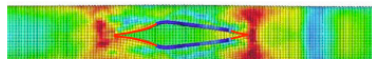
(a)



(a)



(a)



No editorial statement on numerical simulation accuracy. The example is chosen from a number of experiments presumably because the end products looked so much alike. Really nothing else is done to quantify the errors.

Computations were made for two of the Chao and Shepherd [16] experiments of explosively loaded pipes. The finite element model was simply loaded by the pressure time history of the detonation traveling wave; fluid-structure interaction effects were not considered. Nevertheless, the computations reproduce many of the salient features of each experiment and differences in crack paths between two experiments.

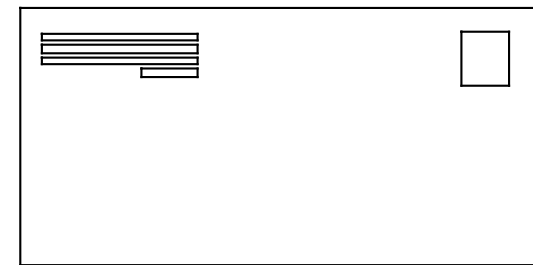


Excerpt from the editorial policy of Physics of Fluids

“Physics of Fluids, published monthly by the American Institute of Physics with the cooperation of the American Physical Society, Division of Fluid Dynamics, is devoted to original theoretical, computational, and experimental contributions to the dynamics of gases, liquids, and complex or multiphase fluids.”

- There is nothing about accuracy, validation, verification, convergence, etc...**
- Everything is in the hands of the editors and reviewers, i.e. the experts.**

I'm not picking on Physics of Fluids,
there are many other examples





Physics of Fluids

PHYSICS OF FLUIDS 21, 051702 (2009)

Turbulent boundary layers up to $Re_\theta=2500$ studied through simulation and experiment

P. Schlatter,^{a)} R. Örlü, Q. Li, G. Brethouwer, J. H. M. Fransson, A. V. Johansson, P. H. Alfredsson, and D. S. Henningson
Linné Flow Centre, KTH Mechanics, SE-100 44 Stockholm, Sweden

(Received 4 March 2009; accepted 24 April 2009; published online 20 May 2009)

The computational domain is $x_L \times y_L \times z_L = 3000 \delta_0^* \times 100 \delta_0^* \times 120 \delta_0^*$ with $3072 \times 301 \times 256$ spectral collocation points in the streamwise, wall-normal, and spanwise directions, respectively. The height and width of the computational domain are chosen to be at least twice the largest 99%

bou
 =25
 the
 with
 unit
 stre
 low
 how
 perf

Neither the experiment or the simulation have any error estimate associated with it. The reader cannot have any idea of the quality of either. Is this an acceptable state of affairs?

sions, but an increased number of grid points as $4096 \times 385 \times 480$ showing only insignificant differences. Statistics are sampled over $\Delta t^+ \approx 24\,000$ viscous time units, or 30 in units of δ_{99}/U_τ at $Re_\theta=2500$. Owing to the high computational cost of the simulations, the code is fully parallelized running on $\mathcal{O}(1000)$ processors.

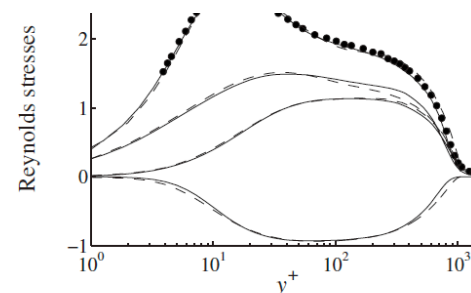
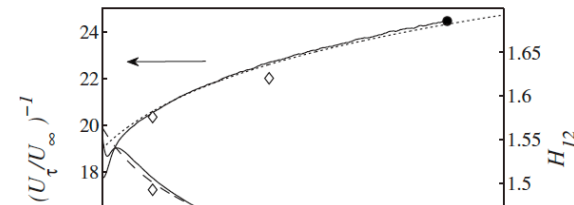


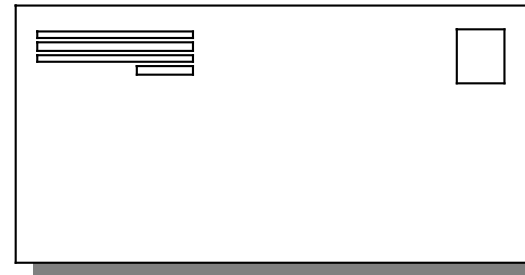
FIG. 3. Turbulent fluctuations u_{rms}^+ , w_{rms}^+ , v_{rms}^+ , and shear stress $\langle u'v' \rangle^+$ (from top). (—) Present DNS at $Re_\theta=2512$, (●) experiments at $Re_\theta=2541$. (---) Correlations based on the attached-eddy hypothesis (Refs. 14–16).



Excerpt from the editorial policy of Journal of Fluid Mechanics

“Journal of Fluid Mechanics is the leading international journal in the field and is essential reading for all those concerned with developments in fluid mechanics. It publishes authoritative articles covering theoretical, computational and experimental investigations of all aspects of the mechanics of fluids. Each issue contains papers on both the fundamental aspects of fluid mechanics, and their applications to other fields such as aeronautics, astrophysics, biology, chemical and mechanical engineering, hydraulics, meteorology, oceanography, geology, acoustics and combustion.”

- **There is nothing about accuracy, validation, verification, convergence, etc...**
- **Everything is in the hands of the editors and reviewers, i.e. the experts.**



Example 2: Journal of Fluid Mechanics

J. Fluid Mech. (2009), vol. 628, pp. 43–55. © 2009 Cambridge University Press
doi:10.1017/S0022112009006156 Printed in the United Kingdom

43

Experimental and numerical study of miscible Faraday instability

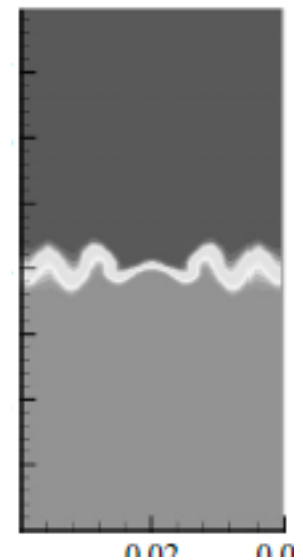
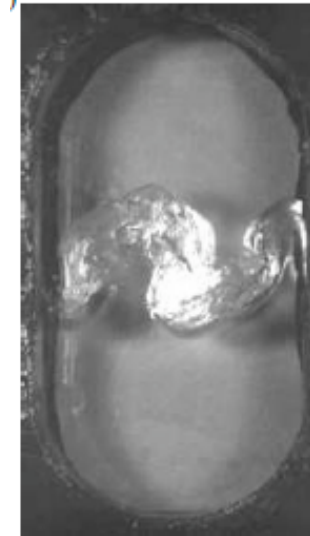
F. ZOUESHTIAGH¹†, S. AMIROUDINE²
AND R. NARAYANAN³

¹Institut d'Electronique, de Microélectronique et de Nanotechnologie UMR CNRS 8520,
Avenue Poincaré, 59652 Villeneuve d'Ascq, France

²LPMI-Arts et Métiers ParisTech., 2 Bd du Ronceray, BP 93525, 49035 Angers, France

³University of Florida, Department of Chemical Engineering,
Gainesville, FL 32611-6005, USA

Equations (3.1) and (3.2) are solved with a finite volume method using the SIMPLER algorithm (Patankar 1980; Amiroudine *et al.* 1997) in a staggered mesh. The space discretization uses the power-law scheme (Patankar 1980) and time discretization is of the first-order Euler type. As the characteristic time t_0 and consequently the characteristic length, which is the diffusive length, are assumed to be



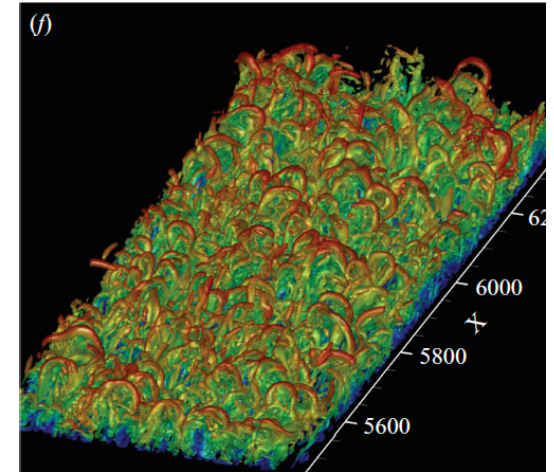
Again both simulation and experiment have no errors estimates. Even the viewgraph norm of the image isn't very convincing. Another telling characteristic is that the simulation is described in very general and vague terms. More importantly the methods used are very old and not very good in modern terms (1st order!!! How is this good enough?).



Direct numerical simulation of turbulence in a nominally zero-pressure-gradient flat-plate boundary layer

XIAOHUA WU¹ AND PARVIZ MOIN^{2†}

The finite-difference grid size is $4096 \times 400 \times 128$ along the x , y and z directions, respectively. Simulation with a coarser grid of $2048 \times 400 \times 128$ was also performed but not presented in this paper. We found that the profile of the skin-friction coefficient C_f obtained from the coarse grid calculation agreed with that from the fine grid to within 0.5% for the turbulent region $730 < Re_\theta < 930$. Agreement is also excellent in the early transitional region for $80 < Re_\theta < 170$, with a maximum deviation of less than 0.05%.



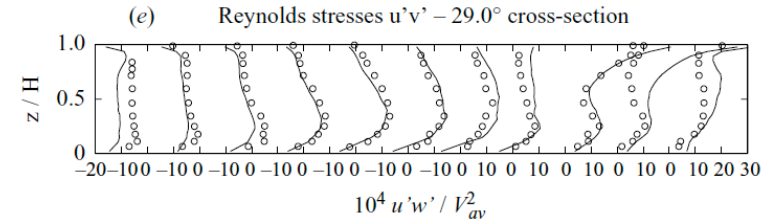
This paper is far better from a V&V perspective than the other JFM papers. The method is described a bit more than other papers. They use two grids! There is a vague error estimate, but no convergence rate. Again, the experimental data is not characterized.



Large-eddy simulation of a mildly curved open-channel flow

W. VAN BALEN^{1†}, W. S. J. UIJTTEWAAL¹
AND K. BLANCKAERT^{1,2}

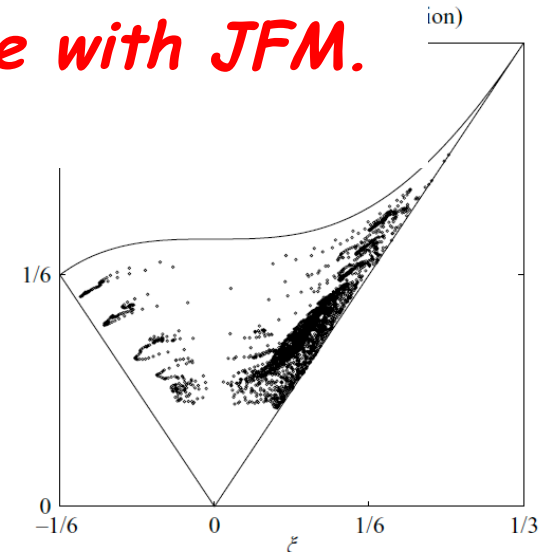
The equations are solved on a staggered mesh using the finite-volume method, with typical grid cells as shown in figure 3, using a pressure-correction algorithm. These equations are numerically integrated in space using the midpoint rule. As a matter of fact, this procedure results in the spatial discretization of the domain following the second-order central scheme. The equations are integrated in time using the explicit second-order Adams–Bashforth scheme. More details on the numerics can be found



This paper is sort of par for the course with JFM. Until...

	Subgrid-scale model	F_i	Boundary conditions	Mesh
Run 1	standard Smagorinsky	0	Non-periodic	$3600 \times 168 \times 24$
Run 2	standard Smagorinsky	0	Periodic	$300 \times 168 \times 24$
Run 3	dynamic Smagorinsky	$\partial p / \partial x_i$	Periodic	$300 \times 168 \times 24$
Run 4	standard Smagorinsky	0	Periodic	$300 \times 168 \times 24$
Run 5	dynamic Smagorinsky	$\partial p / \partial x_i$	Periodic	$300 \times 168 \times 24$

TABLE 2. Model settings for the different runs. F_i refers to (2.11), the mesh is given as the number of grid cells in streamwise, transverse and vertical direction.





A bonus: same article!

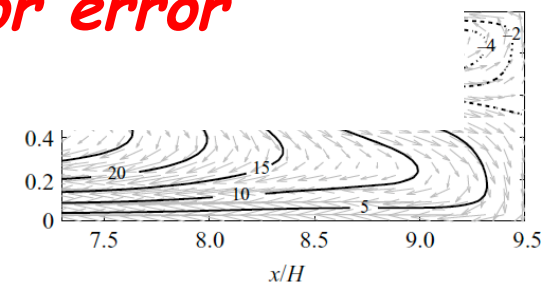
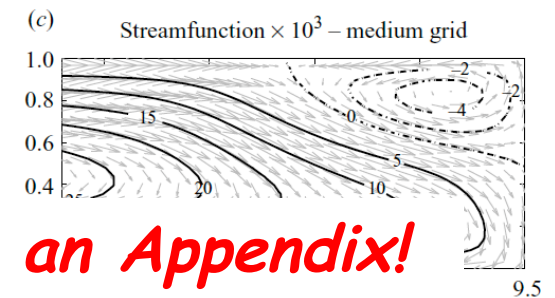
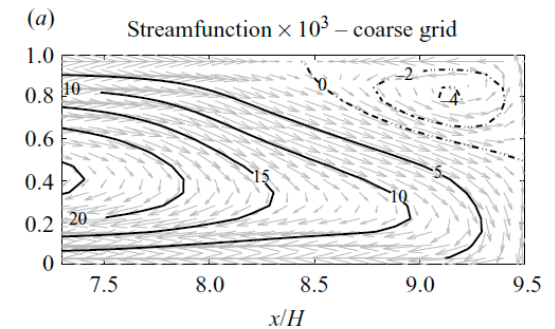
Appendix B. Mesh independency

In order to prove that the solutions of the presented simulations are independent of the mesh, Run 2 from the paper is chosen to be simulated on two other meshes: a coarser mesh and a finer mesh. Recall that Run 2 is the simulation of the axisymmetric flow in the far field of the flow set-up (see figure 5). The big advantage of axisymmetric flow is that periodic boundary conditions can be applied in streamwise direction, thus saving much computational time. An instantaneous result of Run 2, shown in figure 17, also shows the dimensions of the computational domain.

The simulations are run on different meshes: a coarse mesh ($112 \times 200 \times 16$), a medium mesh ($168 \times 300 \times 24$) and a fine mesh ($252 \times 460 \times 36$). The results for the streamfunction ψ and the Reynolds stresses $\overline{u'w'}$ of the three simulations are shown in figure 21 for the outer bank region.

In the background of the pictures in figure 21 the velocity vectors are shown. For this purpose, the velocity fields of the medium and the fine mesh are interpolated to the grid of the coarse mesh to make the comparison comprehensible. It is clearly seen

***A mesh refinement study is included in an Appendix!
They even use three grids, but then let us down by
not even giving us a convergence rate or error
estimate. So close, yet so far!***



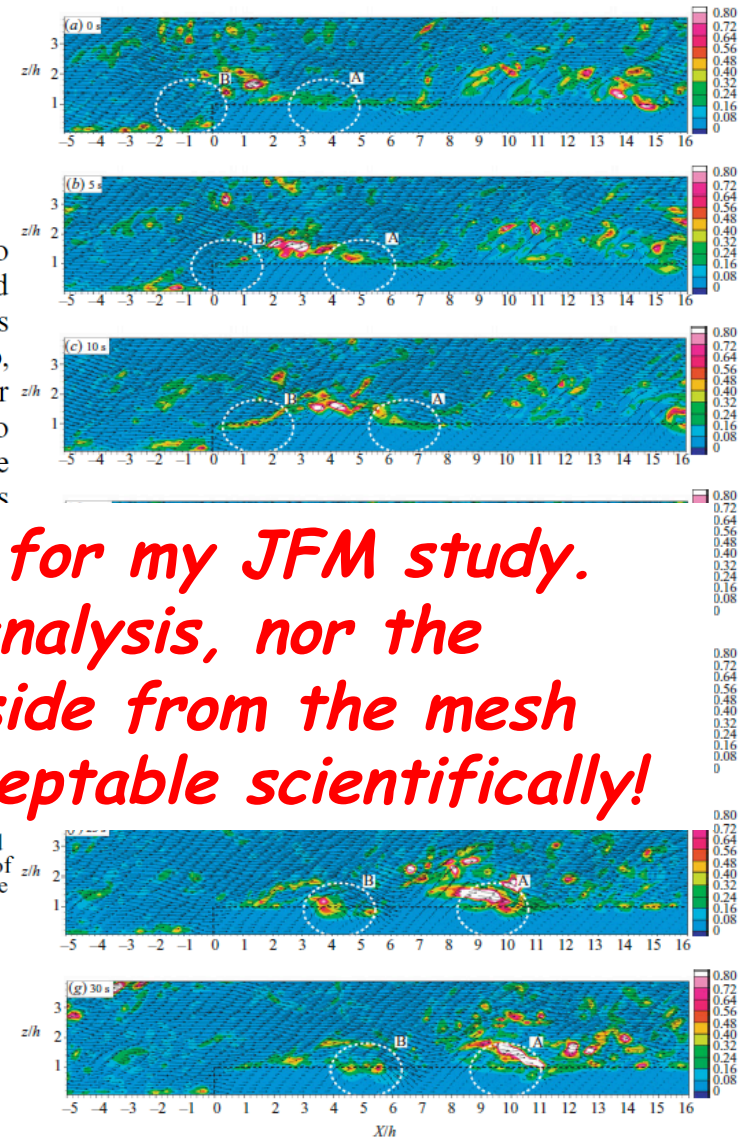
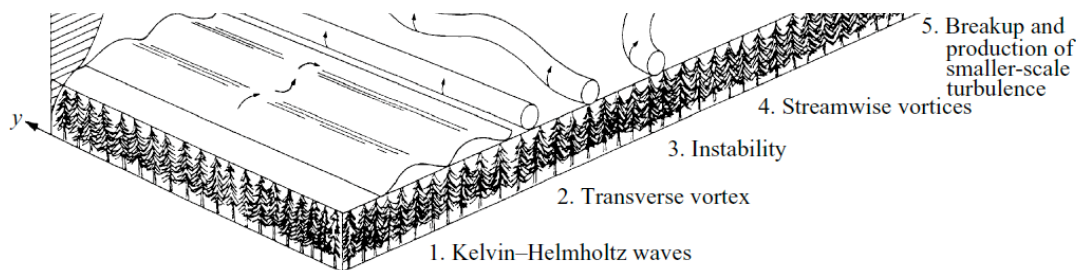


Coherent structures in canopy edge flow: a large-eddy simulation study

S. DUPONT† AND Y. BRUNET

The computational domain extends over $668 \times 200 \times 200 \text{ m}^3$, corresponding to $345 \times 100 \times 65$ grid points in the x -, y - and z -direction, respectively, with 2 m grid spacing below $z = 84 \text{ m}$ and a vertically stretched grid above. This resolution allows us to simulate turbulent structures induced by the mean shear at the canopy top, since their horizontal size is of the order of h , and their vertical size of the order of $h/3$ (Finnigan 2000). The limitation of the vertical size of the domain due to computational time considerations does not allow large mesoscale structures to be resolved. This should not have noticeable consequences on the main results of this

This paper is really the low point for my JFM study. There isn't even a hint of error analysis, nor the merest description of the code aside from the mesh used. I can't see how this is acceptable scientifically!



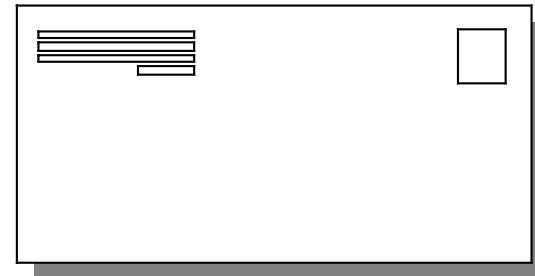


Excerpt from the editorial policy of Physical Review Letters

“Physical Review Letters, published by the American Physical Society, is charged with providing rapid publication of short reports of important fundamental research in all fields of physics. The journal should provide its diverse readership with coverage of major advances in all aspects of physics and of developments with significant consequences across subdisciplines. Letters should therefore be of broad interest. ”

“Mathematical and computational papers that do not have application to physics are generally not suitable for Physical Review Letters.”

- **There is nothing about accuracy, validation, verification, convergence, etc...**
- **Everything is in the hands of the editors and reviewers, i.e. the experts.**





Example 3: Physical Review Letters

PRL 102, 224101 (2009)

PHYSICAL REVIEW LETTERS

week ending
5 JUNE 2009

Discrete Breathers in a Forced-Damped Array of Coupled Pendula: Modeling, Computation, and Experiment

J. Cuevas,¹ L. Q. English,² P. G. Kevrekidis,³ and M. Anderson²

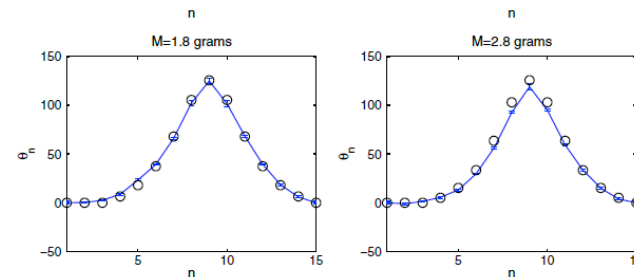
¹Departamento de Física Aplicada I. Escuela Universitaria Politécnica, Universidad de Sevilla.
C/ Virgen de África, 7, 41011 Sevilla, Spain

²Department of Physics & Astronomy, Dickinson College, Carlisle, Pennsylvania 17013, USA

³Department of Mathematics and Statistics, University of Massachusetts, Amherst, Massachusetts 01003-4515, USA
(Received 12 February 2009; published 2 June 2009)

The issues with this paper are simple. The numerical methods are not described, error is not quantified, the experimental data has a small quantified error. The paper reports to put modeling, computing and experiment together yet quantified incompletely although the comparison "looks" good.

comparison of experimental and numerical profiles of stable intersite breathers (middle panels) and on-site breathers (bottom panels). In all cases, $A = 1.12$ cm and $\omega_b = 0.87$. Circles represent the numerical results whereas the full lines with error bars correspond to the experimental profiles.





Electric Field Induced Magnetic Anisotropy in a Ferromagnet

S. J. Gamble,^{1,2} Mark H. Burkhardt,^{2,3} A. Kashuba,⁴ Rolf Allenspach,⁵ Stuart S. P. Parkin,⁶
H. C. Siegmann,¹ and J. Stöhr^{1,3}

¹PULSE Center, Stanford University, Stanford, California 94025, USA

²Department of Applied Physics, Stanford University, Stanford, California 94305, USA

³Stanford Synchrotron Radiation Lightsource, Stanford, California 94305, USA

⁴Bogolyubov Institute for Theoretical Physics 14-b, Metrolohichna Street, Kiev 03680, Ukraine

⁵IBM Research, Zurich Research Laboratory, 8803 Rüschlikon, Switzerland

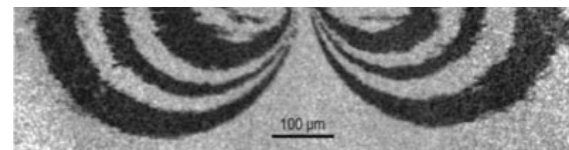
⁶IBM Almaden Research Center, San Jose, California 95120, USA

(Received 8 December 2008; published 27 May 2009)

We report the first observation of a transient all electric field induced magnetic anisotropy in a thin film

This paper was highlighted by this Journal presumably because the picture looks so darn good! This seems like the the viewgraph norm personified. Again, nothing whatsoever is quantified experimentally or computationally.

Fermi's golden rule for the probability to excite a spin wave in second order perturbation. The total dissipation constant is the sum of the intrinsic and the instability terms: $\alpha(t) = \alpha_0 + \alpha_{in}(t)$. The parameters used in the simulation of patterns (b) and (c) in Fig. 3 are $g = 2$, $K_u/K_s = 0.041$, $\gamma = 1.46$, and the intrinsic Gilbert dissipation constant $\alpha_0 = 0.017$. The spin-wave instabilities develop on a time scale ≥ 100 ps, that is long after the bunch has passed. Their inclusion accounts for the observed number of rings and their variable widths.





Science Magazine: Editorial Policy

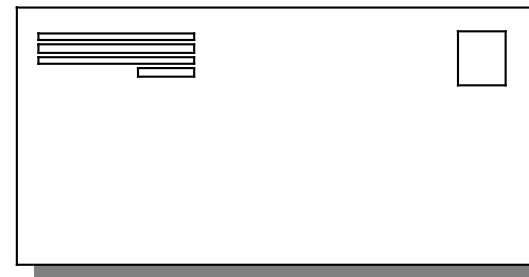
SCIENCE'S MISSION: *Science* seeks to publish those papers that are most influential in their fields and that will significantly advance scientific understanding. Selected papers should present novel and broadly important data, syntheses, or concepts. They should merit the recognition by the scientific community and general public provided by publication in *Science*, beyond that provided by specialty journals.

CRITERIA FOR JUDGMENT

Research Articles should report a major breakthrough in a particular field. They should be in the top 20% of the papers that *Science* publishes and be of strong interdisciplinary interest or unusual interest to the specialist.

Technical Rigor: Evaluate whether, or to what extent, the data and methods substantiate the conclusions and interpretations. If appropriate, indicate what additional data and information are needed to validate the conclusions or support the interpretations.

Supporting Online Material. Supporting online material includes methods, text or data that is of interest only to the specialist, but that is still necessary for the integrity and excellence of the paper. It must be directly related to the conclusions of the print paper. We welcome suggestions for deletions of supporting online material or items that should be moved to supporting online material.





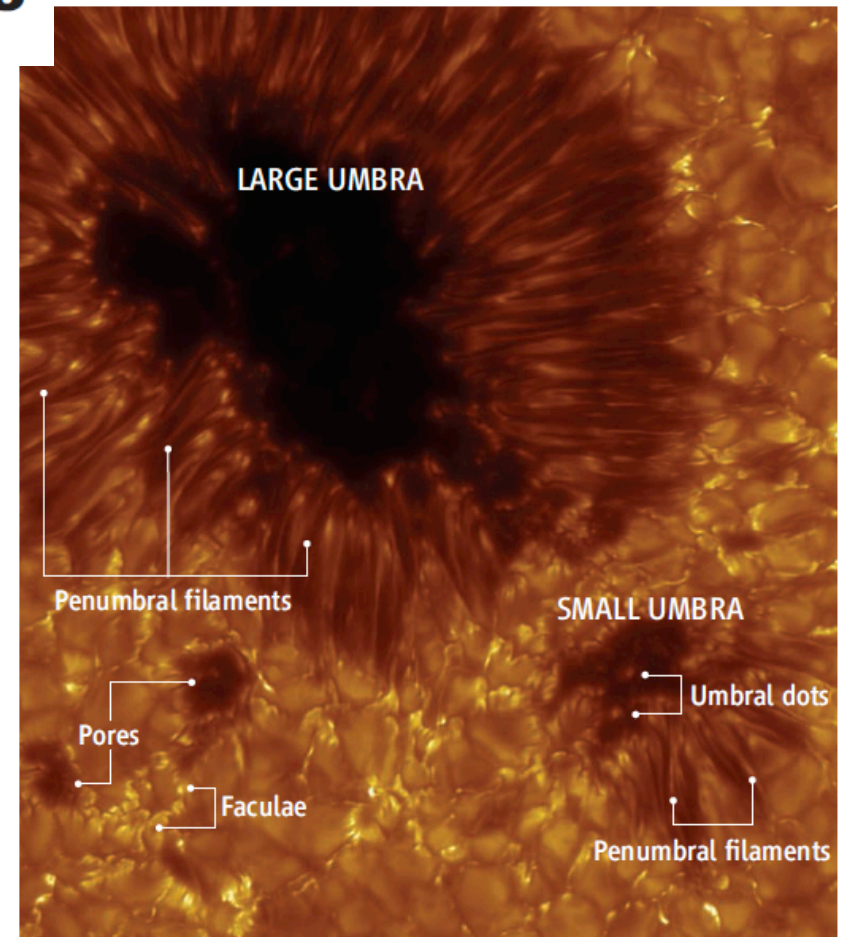
Science often has a “news” article about the research papers.

Sunspot Flows and Filaments

Göran Scharmer

In 1941, Ludwig Biermann recognized that the reduced brightness of sunspot umbrae could be due to suppression of the convective energy flux by their strong magnetic field. But this led to the problem of explaining why sunspots are not completely dark. Simulations of sunspot umbrae (5) demonstrate the formation of narrow plumes within which the magnetic field is expelled by overturning convection, leading to the formation of bright umbral dots.

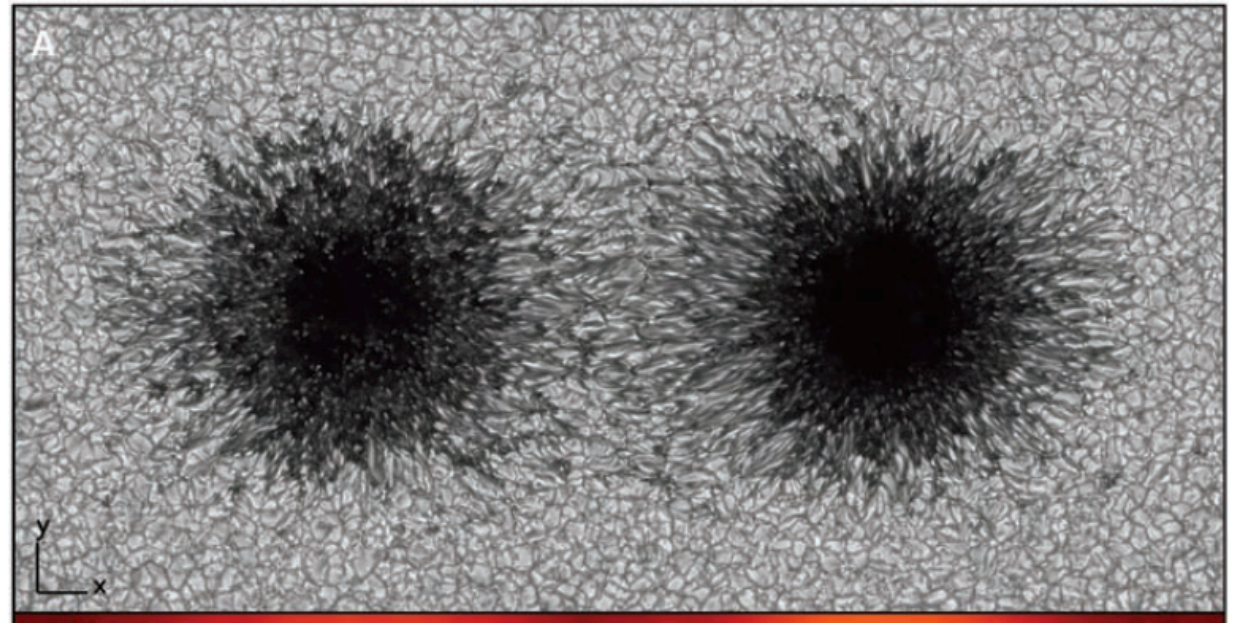
The first 3D simulations of sunspots (10, 11), although limited to azimuthally narrow slices of a sunspot, did provide consistency with several observed aspects of penumbrae. They demonstrated convection in radially aligned sheet-like structures with strongly reduced field strength and systematic (but weak) radial outflows. This led us to the conclusion that the Evershed flow is identical to the horizontal component of penumbral convection (12). Rempel *et al.* now present simulations of two sunspots of opposite polarities and not just thin slices of a sunspot as in the earlier simulations (10, 11). They





The research article in Science.

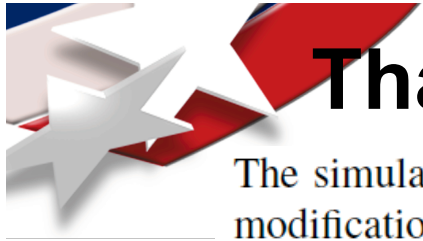
field between the spots. Our numerical box had a horizontal extension of 98 Mm by 49 Mm and a depth of 6.1 Mm. The spatial grid resolution was 32 km in the horizontal directions and 16 km in the vertical. The sunspots evolved for 3.6 hours during the simulation, which was sufficient to study the penumbral structure and dynamics; processes that evolve on longer time scales, such as moat flows, were not fully developed in this simulation. However, the surface evolution of



The strongest "evidence" is the likeness of the above picture with photographs of the actual sun. All the details and evidence of numerical quality is in supplementary material. I decided to look at it.

unioral dots as well as inner and outer penumbrae in terms of magnetoconvection in a magnetic field with varying inclination. Furthermore, a consistent physical picture of all observational characteristics of sunspots and their surroundings is now emerging.

8. More detailed information about the physical model, the numerical code, and the simulation setup is available as supporting material on *Science Online*.



Thank God for supplementary material!

The simulation presented here has been carried out with the *MURaM* MHD code (1, 2), with modifications described in (3). The physics, numerics and boundary conditions are similar to earlier runs described there, the primary difference here is the far larger domain size and the initial magnetic field configuration.

We ran the simulation for the first hour of simulated time with a rather low numerical grid resolution of $96 \times 96 \times 32$ km to get past initial transients. The second hour was performed at a medium resolution of $48 \times 48 \times 24$ km and then followed by another 1.6 hours with a resolution of $32 \times 32 \times 16$ km (corresponding to $3072 \times 1536 \times 384$ grid cells). The results presented here are based on snapshots near the end of the high-resolution run and partly on temporal averages

***Very disappointing! In fact new questions were raised.
The references had to be examined to find any details.
No V or V can be found.***

3. M. Rempel, M. Schüssler, M. Knölker, *ApJ* **691**, 640 (2009).



OK, let's look at those references

There is a little, but not much in the Ap. J. paper.
Let's look at that thesis. There is no V or ν .

This chapter discusses the numerical methods of the MHD code. The code used here is based on a code for general MHD applications, which was developed by T. Linde and A. Malagoli at the University of Chicago. This basic code solves the MHD equations (2.17), (2.19), (2.20), and (2.27) without radiative source term, assuming constant scalar diffusion coefficients μ , K , and η and using the

The MHD code solves the system of MHD equations on a three-dimensional equidistant cartesian grid. The spatial discretization of the equations is based on the fourth-order centered-difference scheme on a 5-point stencil. Choosing i as

The numerical solution of the system is advanced in time using an explicit fourth-

The method is described albeit not specifically. There isn't any verification at all.

separate diffusion coefficient, consisting of a shock-resolving and a hyperdiffusive part, is defined:

$$\nu_l(u) = \nu_l^{\text{shk}} + \nu_l^{\text{hyp}}(u). \quad (3.14)$$

$$\nu_l^{\text{shk}} = \begin{cases} c_{\text{shk}} \cdot \Delta x_l^2 \cdot |\nabla \cdot \mathbf{v}| & \nabla \cdot \mathbf{v} < 0 \\ 0 & \nabla \cdot \mathbf{v} \geq 0 \end{cases}. \quad (3.15)$$

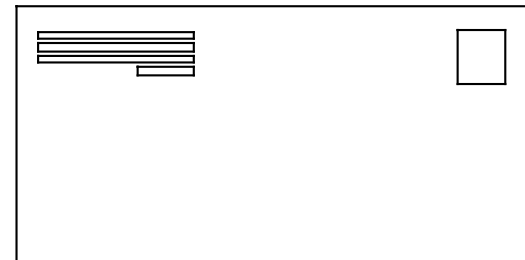
$$\nu_l^{\text{hyp}}(u) = c_{\text{hyp}} \cdot c_{\text{tot}} \cdot \Delta x_l \cdot \frac{\max_3 \Delta_l^3 u}{\max_3 \Delta_l^1 u}. \quad (3.16)$$



nature Magazine

Editorial Guidance: Writing a peer review

- Are the claims convincing? If not, what further evidence is needed?
- Are there other experiments or work that would strengthen the paper further?
- How much would further work improve it, and how difficult would this be? Would it take a long time?
- Should the authors be asked to provide supplementary methods or data to accompany the paper online? (Such data might include source code for modelling studies, detailed experimental protocols or mathematical derivations.)
- Have they provided sufficient methodological detail that the experiments could be reproduced?
- Is the statistical analysis of the data sound, and does it conform to the journal's guidelines?





The proportionality of global warming to cumulative carbon emissions

by H. Damon Matthews, Nathan P. Gillett, Peter A. Stott & Kirsten Zickfeld - Nature 459, 829-832 (11 June 2009) | doi:10.1038/nature08047

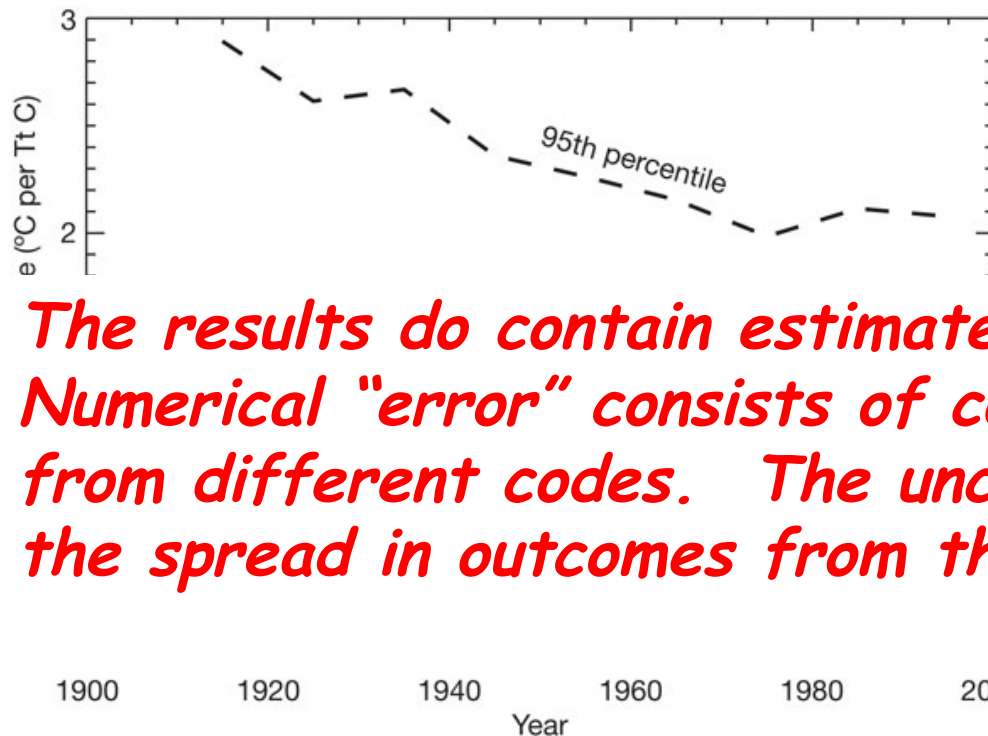
Editor's summary: To date, efforts to describe and predict the climate response to human CO₂ emissions have focused on climate sensitivity: the equilibrium temperature change associated with a doubling of CO₂. But recent research has suggested that this 'Charney' sensitivity, so named after the meteorologist Jule Charney who first adopted this approach in 1979, may be an incomplete representation of the full Earth system response, as it ignores changes in the carbon cycle, aerosols,

Again, the magazine has a laypersons news story plus an Editor's summary of the article. For Nature, all the numerical work that I could find was related to climate change. Its important to note that these papers are significant in terms of much larger geopolitical dynamics with massive economic consequences too.

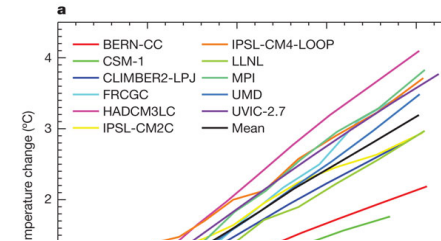


Results

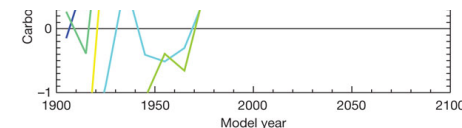
Observational estimates of CCR.



CCR estimated from the C4MIP simulations¹¹.



The results do contain estimates of observational errors. Numerical "error" consists of comparing the results from different codes. The uncertainty is defined as the spread in outcomes from the codes.



HD Matthews *et al.* *Nature* **459**, 829-832 (2009) doi:10.1038/nature08047



Method's summary

METHODS SUMMARY

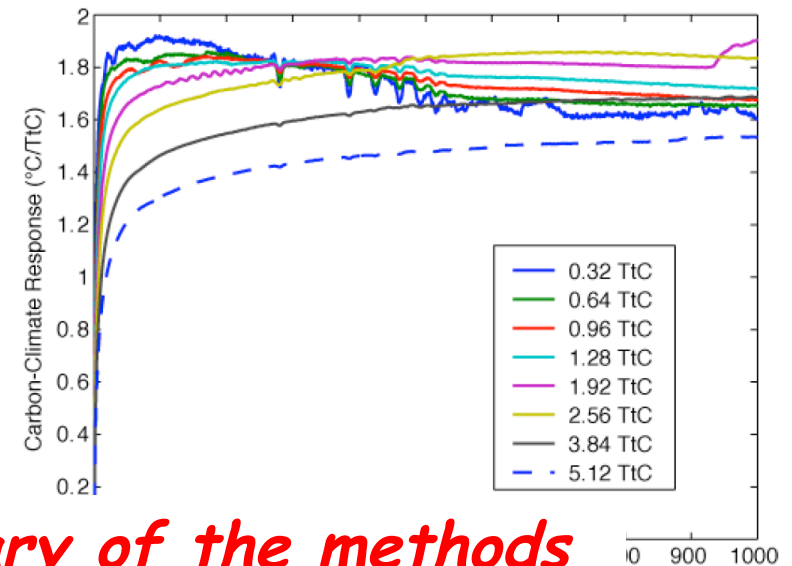
For the idealized model experiments (1% per year CO₂ increase; doubled/quadrupled CO₂) we used the UVic ESCM version 2.8 (refs 9, 18–20). The UVic ESCM is a computationally efficient coupled climate–carbon model, with interactive representations of three-dimensional ocean circulation, atmospheric energy and moisture balances, sea ice dynamics and thermodynamics, dynamic vegetation and the global carbon cycle (including land and both inorganic and organic ocean carbon). Version 2.7 of the UVic ESCM was one of the 11 participating models in C4MIP¹¹, in which models were driven by a common CO₂ emissions scenario and carbon sinks and atmospheric CO₂ concentrations were calculated interactively until the year 2100. From the C4MIP simulations, we estimated CCR using globally averaged temperature change and accumulated carbon emissions at the year of CO₂ doubling in each simulation.

Our observational estimate of CCR was derived using estimates of CO₂-attributable warming and cumulative CO₂ emissions for each decade of the twentieth century relative to 1900–09. We estimated CO₂-attributable warming using an

The paper also includes a summary of the methods used plus online supplementary materials.

distributed uncertainties for radiative forcings and greenhouse-gas efficacy, respectively²². We calculated cumulative carbon emissions from fossil fuels and land-use change^{13,14,23}, and assumed a one-sigma systematic uncertainty on land-use emissions of ± 0.5 PgC per year²⁴. Our central estimates for CO₂-attributable warming and cumulative emissions at 1990–99 relative to 1900–09 were 0.492 °C and 0.338 TtC, respectively. We calculated a probability density function for CCR based on the probability distributions of the constituent terms, which we used to estimate the mean and the 5th and 95th percentiles.

Full Methods and any associated references are available in the online version of the paper at www.nature.com/nature.



ed, simulated by the

UVic ESCM in response to instantaneous pulse-carbon emissions from 0.32 to 5.12 TtC, followed by zero additional emissions. On timescales of 20 to 1000 years, and for emissions up to about 2 TtC, the instantaneous temperature response per unit carbon emitted is between about 1.6 and 1.9 °C/TtC.



C4MIP?

Journal of Climate Article: Volume 19, Issue 14 (July 2006) pp. 3337–3353
 Climate–Carbon Cycle Feedback Analysis: Results from the C4MIP Model Intercomparison

P. Friedlingstein, L. Bopp, P. Rayner P. Cox R. Betts, C. Jones W. von Bloh, V. Brovkin P. Cadule, S. Doney, M. Eby, H. D. Matthews, A. J. Weaver, I. Fung J. John, G. Bala, F. Joos K. Strassmann, T. Kato, M. Kawamiya, C. Yoshikawa, W. Knorr, K. Lindsay, H. D. Matthews, T. Raddatz and C. Reick, E. Roeckner, K.-G. Schnitzler, R. Schnur, and N. Zeng,

Models	Atmosphere	Ocean	Land carbon	DGVM	Ocean carbon	References
HadCM3LC	HADCM3 2.5° × 3.75°, L19	2.5° × 3.75°, L20 flux adjustment	MOSES/TRIFFID	Yes	HadOCC	Cox et al. (2000)
IPSL-CM2C	LMD5 64 × 50, L19 (5° × 4°)	OPA-7, 2° × 2°, L31 no flux adjustment	SLAVE	No	NPZD	Dufresne et al. (2002)
IPSL-CM4-LOOP	LMDZ-4 96 × 72, L19 (3° × 3)	ORCA2, 2° × 2°, L31, no flux adjustment	ORCHIDEE	Not here	PISCES	Marti et al. (2005) Krinner et al. (2005) Aumont et al. (2003)
CSM-1	CCM3 T31, L18	NCOM 3.6° lon 0.8–1.8° lat	LSM, CASA	No	OCMIP-biotic	Doney et al. (2006); Fung et al. (2005)
MPI	ECHAM5, T63, L31	MPI-OM, 1.5°, L40, no flux adjustment	JSBACH	No	HAMOCC5	Raddatz et al. (2005, unpublished manuscript)
LLNL FRCGC	CCM3, 2.8° × 2.8°, L18 CCSR/NIES/FRCGC T42(2.8° × 2.8°), L20	POP 0.6° × 0.6°, L40 COCO No flux adjustment, (0.5°–1.4°) × 1.4°, L20	IBIS, flux adjustment Sim-CYCLE	Yes No	OCMIP NPZD	Thompson et al. (2004)
UMD UVic-2.7	QTCM 5.6° × 3.7° EMBM 1.8° × 3.6°	Slab mixed layer, 5.6° × 3.7° Mom 2.2, 1.8° × 3.6°, L19, no flux adjustment	VEGAS MOSES/TRIFFID	Yes Yes	Three-box model OCMIP Abiotic	Zeng et al. (2004) Meissner et al. (2003)
CLIMBER2-LPJ	2.5-D, 10° × 51° statistical-dynamical	Zonally averaged, 2.5°lat, 3 basins	LPJ	Yes	NPZD	Matthews et al. (2005a) Brovkin et al. (2004) Sitch et al. (2005)
BERN-CC	EBM 2.5° × 3.75°	HILDA box-diffusion model	LPJ	Yes	Perturbation approach	Joos et al. (2001) Gerber et al. (2003)



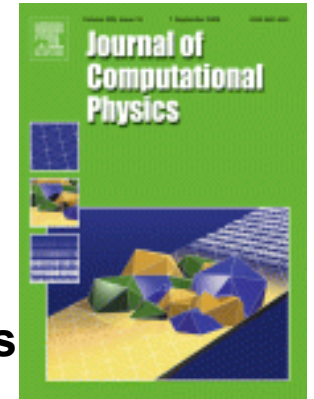
“The plural of ‘anecdote’ is not ‘evidence’.”
Alan Leshner, publisher of Science

***“...what can be asserted without evidence can
also be dismissed without evidence.”***

by Christopher Hitchens



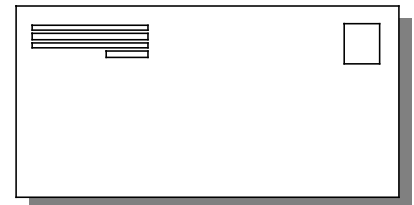
Journal of Computational Physics



Journal of Computational Physics thoroughly treats the computational aspects of physical problems, presenting techniques for the numerical solution of mathematical equations arising in all areas of physics. The journal seeks to emphasize methods that cross disciplinary boundaries.

Elsevier's reviewer guidance:

- Is the **methodology** appropriate? Does it accurately explain how the data was collected? Is the design suitable for answering the question posed? Is there sufficient information present for you to replicate the research? Does the article identify the procedures followed? Are these ordered in a meaningful way? If the methods are new, are they explained in detail? Was the sampling appropriate? Have the equipment and materials been adequately described? Does the article make it clear what type of data was recorded; has the author been precise in describing measurements?
- **Results:** this is where the author/s should explain in words what he/she discovered in the research, any interpretation should not be included in this section. The results should be clearly laid out and in a logical sequence. You will need to consider if the appropriate analysis been conducted. Are the statistics correct? If you are not comfortable with statistics, advise the editor when you submit your report.

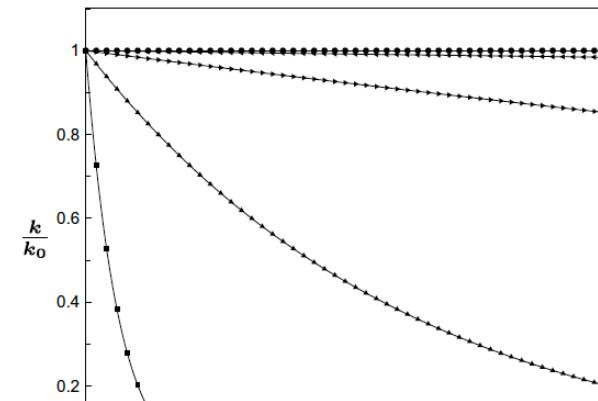


A fully discrete, kinetic energy consistent finite-volume scheme for compressible flows

Pramod K. Subbareddy*, Graham V. Candler

Department of Aerospace Engineering and Mechanics, University of Minnesota, 107, Akerman Hall, 110, Union Street, Minneapolis, MN 55455, United States

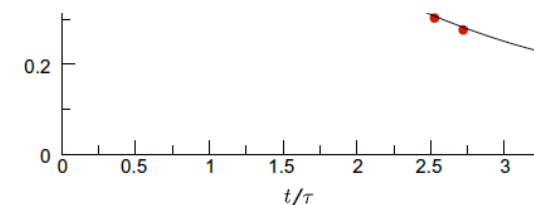
A robust, implicit, low-dissipation method suitable for LES/DNS of compressible turbulent flows is discussed. The scheme is designed such that the discrete flux of kinetic energy and its rate of change are consistent with those predicted by the momentum and continuity equations. The resulting spatial fluxes are similar to those derived using the so-called skew-symmetric formulation of the convective terms. Enforcing consistency for the time derivative results in a novel density weighted Crank–Nicolson type scheme. The method is stable without the addition of any explicit dissipation terms at very high Reynolds numbers for flows without shocks. Shock capturing is achieved by switching on a dissipative flux term which tends to zero in smooth regions of the flow. Numerical examples include a one-dimensional shock tube problem, the Taylor–Green problem, simulations of isotropic turbulence, hypersonic flow over a double-cone geometry, and compressible turbulent channel flow.



The papers are filled with exquisite detail on the numerical method. The V&V of the method still leaves a lot to be desired. The calculations were all done on a single mesh resolution. Errors are not shown nor discussed. Many papers in JCP do actually achieve a much higher standard.

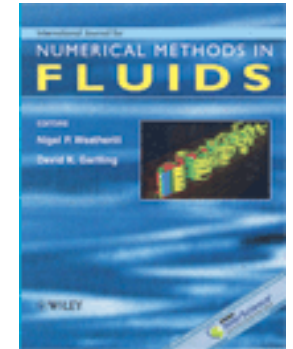


Fig. 3. Double-cone in hypersonic flow. (a) Temperature contours (1024 × 512 grid). Inset shows the numerical shadowgraph of the shock interaction region. (b) Heat transfer rate at the surface. Symbols: experiment, solid line: computation.





International Journal for Numerical Methods in Fluids



The continual increase in computing capability has enabled applied mathematicians, engineers and scientists to achieve solutions to complex problems with ever-increasing accuracy and make significant progress in the solution of previously intractable problems. This trend is particularly significant in fluid mechanics, where computer simulation is now a significant element in flow analysis and scientific discovery over many areas of investigation...

...Manuscripts in which the primary contribution is experimental or analytical are also encouraged, if such results are compared with previously published numerical predictions or are of sufficient detail to serve as components of verification/validation. ...



Drag reduction by flow separation control on a car after body

Mathieu Rouméas¹, Patrick Gilliéron¹ and Azeddine Kourta^{2,*},†

¹*Groupe 'Mécanique des Fluides et Aérodynamique', Direction de la recherche Renault,
1, avenue du Golf (TCR AVA 058), 78288 Guyancourt, France*

²*Institut de Mécanique des Fluides de Toulouse, Groupe EMT2 Avenue du professeur Camille Soula,
31000 Toulouse, France*

New development constraints prompted by new pollutant emissions and fuel consumption standards (Corporate Average Economy Fuel) require that automobile manufacturers develop new flow control devices capable of reducing the aerodynamic drag of motor vehicles. The solutions envisaged must have a negligible impact on the vehicle geometry. In this context, flow control by continuous suction is seen as a promising alternative. The control configurations identified during a previous 2D numerical analysis are adapted for this purpose and are tested on a 3D geometry. A local suction system located on the upper part of the rear window is capable of eliminating the rear window separation on simplified fastback car geometry. Aerodynamic drag reductions close to 17% have been obtained. Copyright © 2008 John Wiley & Sons Ltd

What is the mesh? This is absolutely unbelievable!

numerical models and mesoscopic kinetic equations. The fundamental principle of the LBM is to construct simplified kinetic models that incorporate the essential physics of microscopic or mesoscopic processes such that the macroscopic-averaged properties conform to the desired macroscopic equations. The basic premise for using these simplified kinetic-type methods for macroscopic fluid flows is that the macroscopic fluid dynamics are the result of the collective behaviour of many microscopic particles in the system and that the macroscopic dynamics are not sensitive to the underlying details as is the case in microscopic physics [17, 18].

As in the case of all numerical space–time discretization methods, the LBM is not capable of resolving all turbulence scales. The computation code, therefore, uses a turbulence model, which introduces a turbulent viscosity into the initial model. The turbulence model is the RNG k – ε model originally developed by Yakhot and Orszag [24]. The equations describing the transport of kinetic energy and dissipation applied by the model are resolved on the same lattice as the Boltzmann equations. The discretization diagram used is a second order in space (Lax–Wendroff finite difference model) associated with a time-explicit integration diagram [25]. Close to the wall, a specific velocity law is applied to limit the computational workload [25]. The velocity is then described by a logarithmic law.

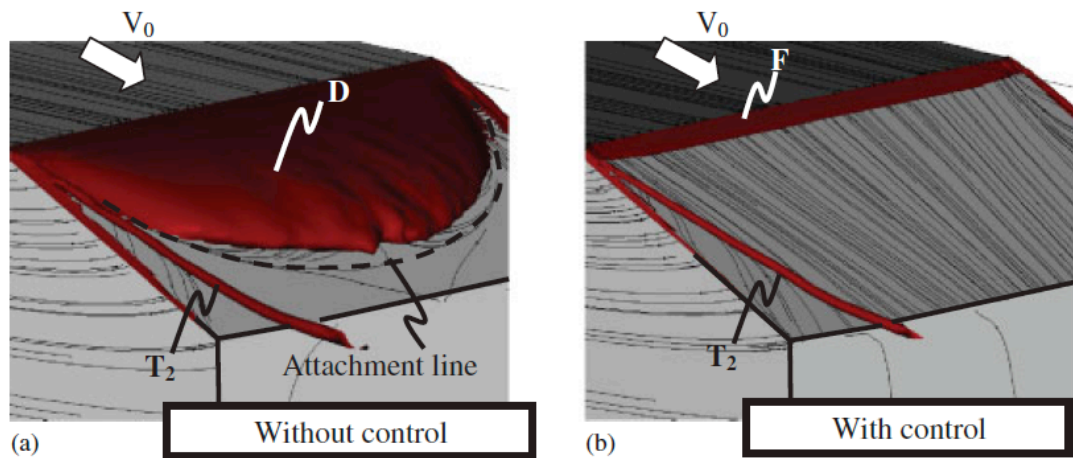
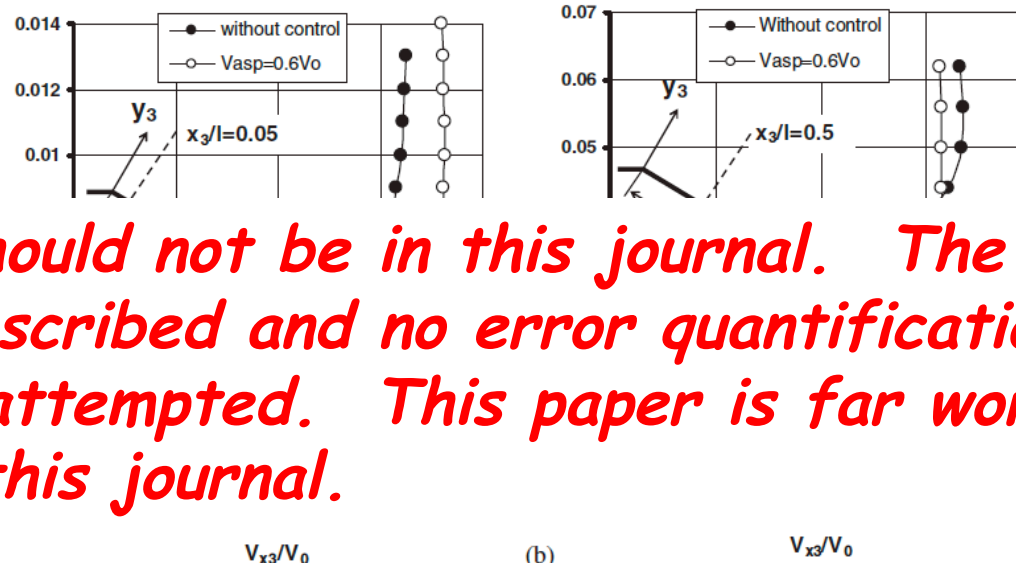


Figure 3. Total pressure loss iso-surfaces ($C_{pi} = 1, 22$) and friction line traces on rear window: (a) without control and (b) with suction.



This paper should not be in this journal. The calculations are poorly described and no error quantification or validation is attempted. This paper is far worse than average for this journal.

These solutions are currently being analysed and offer a notable potential for reducing aerodynamic drag and automobile fuel consumption. The results presented in this paper confirm the potential of active suction control in the automobile industry. The results should, however, be corroborated by experimental results and tested on real car flow configuration.



INTERNATIONAL JOURNAL FOR NUMERICAL METHODS IN FLUIDS

Int. J. Numer. Meth. Fluids 2009; 60:1259–1288

Published online 17 November 2008 in Wiley InterScience (www.interscience.wiley.com). DOI: 10.1002/flid.1934

Quantitative benchmark computations of two-dimensional bubble dynamics

S. Hysing^{1,*}, S. Turek², D. Kuzmin², N. Parolini³, E. Burman⁴, S. Ganesan⁵
and L. Tobiska⁶

¹*Universitat Politècnica de Catalunya (UPC), Jordi Girona 1-3, Edifici C1, 08034 Barcelona, Spain*

²*Institut für Angewandte Mathematik, TU Dortmund, Vogelpothsweg 87, 44227 Dortmund, Germany*

³*MOX, Dipartimento di Matematica, Politecnico di Milano, Via Bonardi 29, 20133 Milano, Italy*

⁴*Department of Mathematics, University of Sussex, Brighton BN1 9RF, U.K.*

⁵*Department of Aeronautics, Imperial College, London, U.K.*

⁶*Institut für Analysis und Numerik, Otto-von-Guericke Universität, 39016 Magdeburg, Germany*

Benchmark configurations for *quantitative* validation and comparison of incompressible interfacial flow codes, which model two-dimensional bubbles rising in liquid columns, are proposed. The benchmark quantities: circularity, center of mass, and mean rise velocity are defined and measured to monitor convergence toward a reference solution. Comprehensive studies are undertaken by three independent research groups, two representing Eulerian level set finite-element codes and one representing an arbitrary Lagrangian–Eulerian moving grid approach.

The first benchmark test case considers a bubble with small density and viscosity ratios, which undergoes moderate shape deformation. The results from all codes agree very well allowing for target reference values to be established. For the second test case, a bubble with a very low density compared to that of the surrounding fluid, the results for all groups are in good agreement up to the point of break up, after which all three codes predict different bubble shapes. This highlights the need for the research community to invest more effort in obtaining reference solutions to problems involving break up and coalescence.

Other research groups are encouraged to participate in these benchmarks by contacting the authors and submitting their own data. The reference data for the computed benchmark quantities can also be supplied for validation purposes. Copyright © 2008 John Wiley & Sons, Ltd.

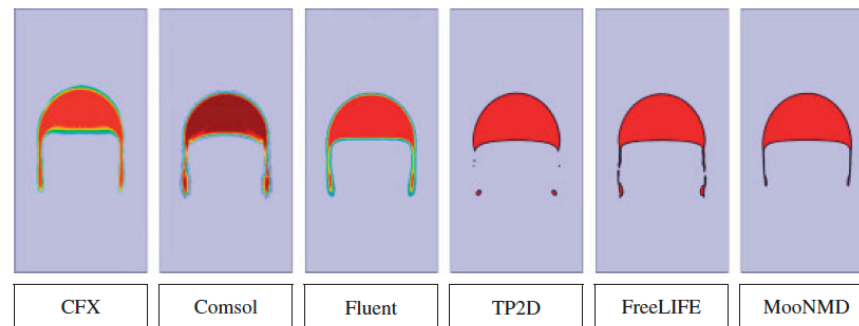
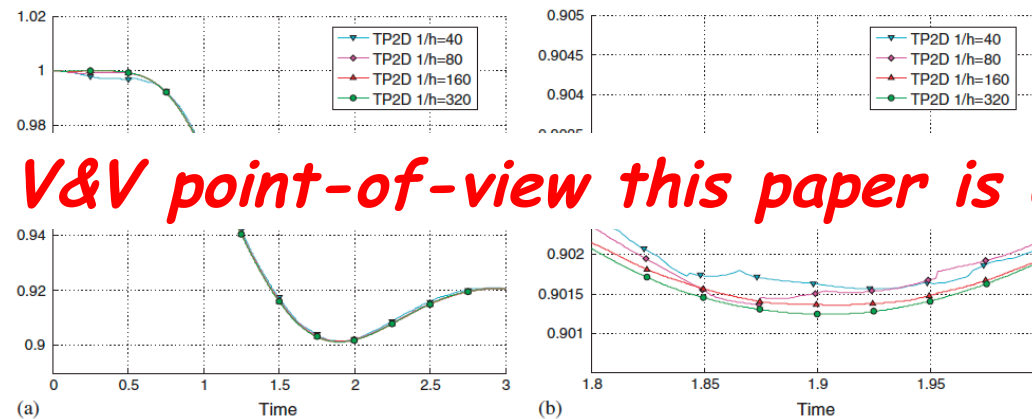




Table IV. Relative error norms and convergence orders for test case 1 and group 1 (TP2D).

$1/h$	$\ e\ _1$	ROC ₁	$\ e\ _2$	ROC ₂	$\ e\ _\infty$	ROC _∞
<i>Circularity</i>						
40	1.00e-03		1.22e-03		2.89e-03	
80	3.01e-04	1.74	3.63e-04	1.75	9.67e-04	1.58
160	8.83e-05	1.77	1.10e-04	1.72	4.32e-04	1.16
<i>Center of mass</i>						
40	2.65e-03		2.99e-03		3.56e-03	
80	9.64e-04	1.46	1.02e-03	1.55	1.14e-03	1.64
160	2.62e-04	1.88	2.71e-04	1.91	2.96e-04	1.95
<i>Rise velocity</i>						
40	1.19e-02		1.29e-02		1.49e-02	
80	2.90e-03	2.04	3.07e-03	2.07	5.08e-03	1.55
160	7.73e-04	1.91	7.85e-04	1.97	1.94e-03	1.39

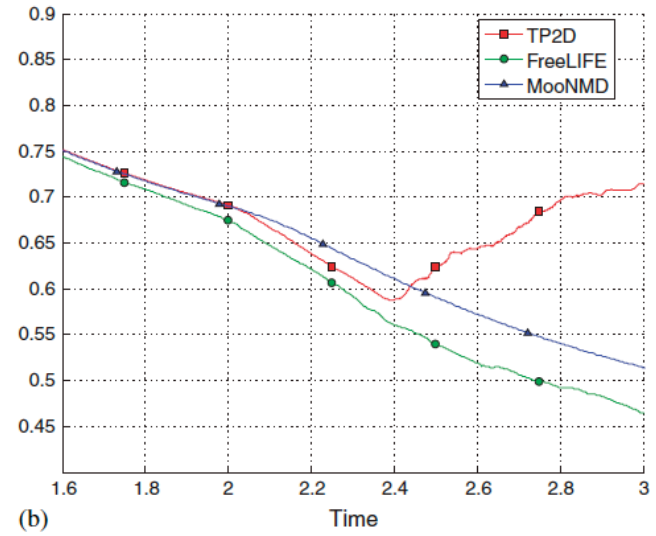
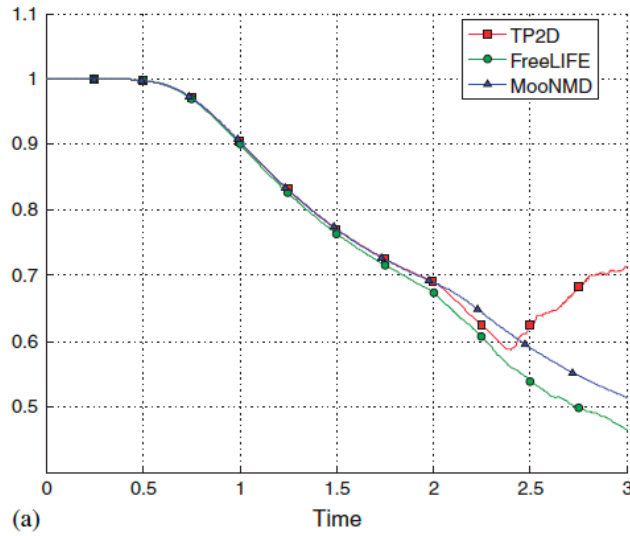
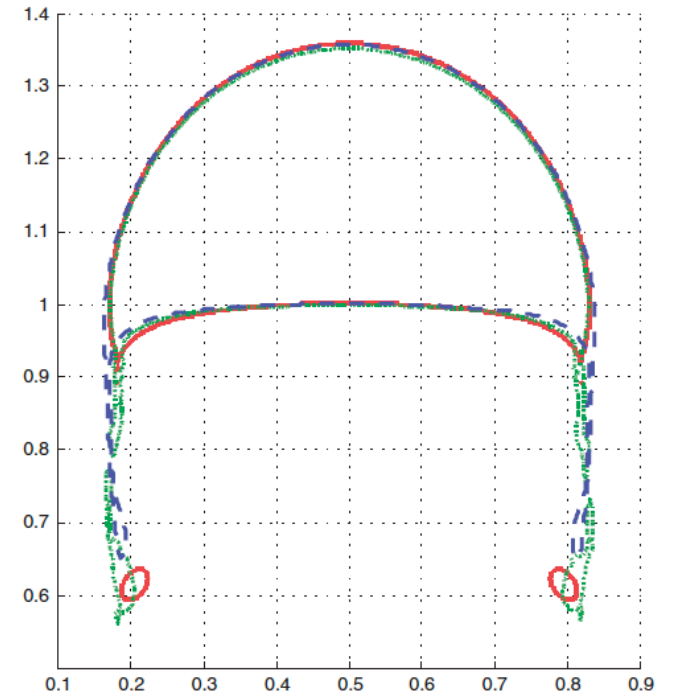
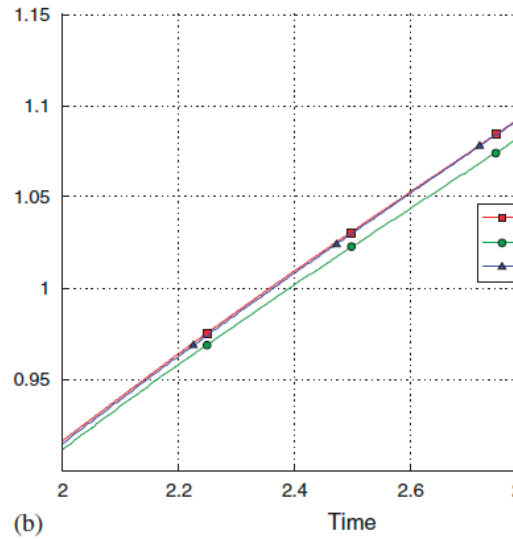
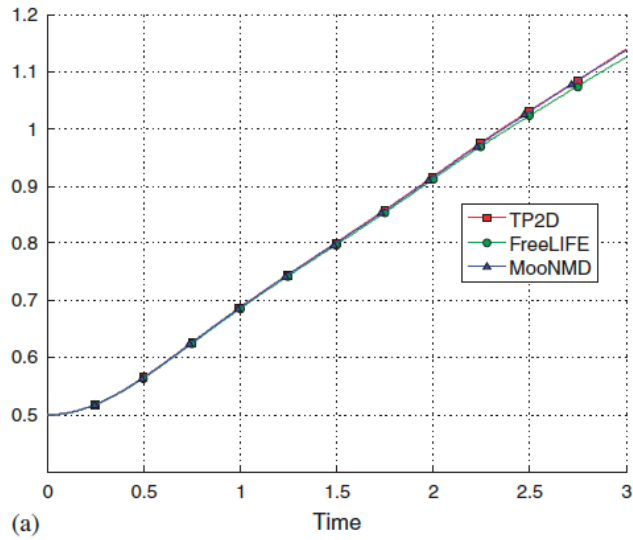


Wow! From a V&V point-of-view this paper is awesome!

Figure 4. Circularity for test case 1 and group 1 (TP2D): (a) circularity and (b) close-up of the circularity.

Table V. Minimum circularity and maximum rise velocity, with corresponding incidence times, and the final position of the center of mass for test case 1 and group 1 (TP2D).

$1/h$	40	80	160	320
ϕ_{\min}	0.9016	0.9014	0.9014	0.9013
$t \phi=\phi_{\min}$	1.9234	1.8734	1.9070	1.9041
$V_{c,\max}$	0.2418	0.2418	0.2419	0.2417
$t V_c=V_{c,\max}$	0.9141	0.9375	0.9281	0.9213
$y_c(t=3)$	1.0818	1.0810	1.0812	1.0813





Let's move into nuclear engineering!



Contents lists available at ScienceDirect

Nuclear Engineering and Design

journal homepage: www.elsevier.com/locate/nucengdes



Numerical and modeling issues in application of CFD to flow in a simplified plenum relevant to a prismatic VHTR

Ertan Karaismail, Ismail Celik*

Mechanical and Aerospace Engineering, West Virginia University, Morgantown, WV 26506-6106, USA

ABSTRACT

Computational Fluid Dynamics (CFD) calculations have been performed for turbulent flow inside a plenum model that resembles a section of the lower plenum of a typical helium-cooled prismatic Very High Temperature Reactor (VHTR). Different Reynolds Averaged Navier–Stokes (RANS) based turbulence models are employed to investigate the capability in capturing unsteady large scale coherent structures

d
tl
q
ei
P
n
a:
ai
la
procedures.

**From a V&V point of view, there are a lot of good signs!
I see a set of three grids, but the description of the
solution methodology leaves a lot to be desired.**

© 2010 Elsevier B.V. All rights reserved.

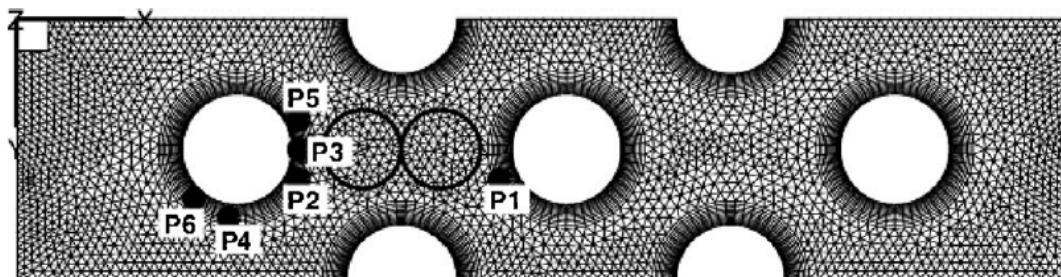
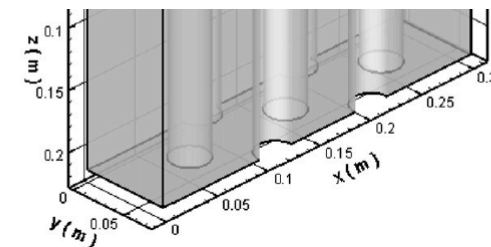
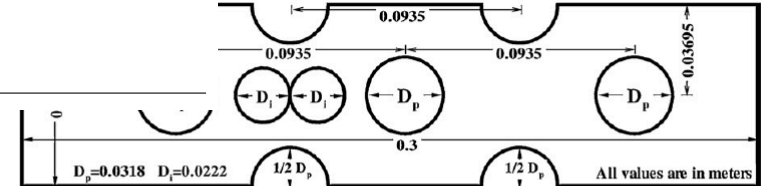


Fig. 3. Coarse grid details.





The flowing medium is liquid water with a density, ρ , of 998 kg/m^3 and dynamic viscosity μ of $1.0 \times 10^{-3} \text{ kg/ms}$. The

sim
and
sing
jets

flow
bul
ple
wit

Stress transport (SST) $k-\omega$ models were performed to simulate the turbulent flow. These turbulence models were selected after tedious preliminary simulations with the several other models (Celik, 2007a). In the present study, the URANS calculations are based on the well-developed approach of moving average (Lumley

In the interest of accuracy, convective and diffusive terms were discretized with second order upwind and second order central discretization schemes, respectively. On the other hand, first order time discretization with a sufficiently small step size ($1 \times 10^{-3} \text{ s}$; ca. $1/25,000$ of computed vortex shedding period) is used. The iterative convergence criteria used at every time step was based on sum of

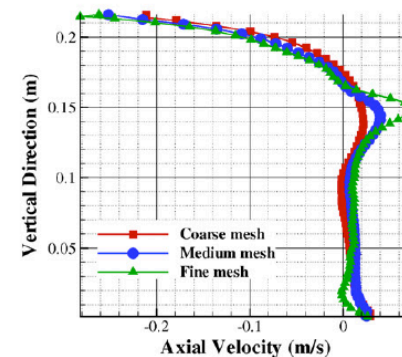
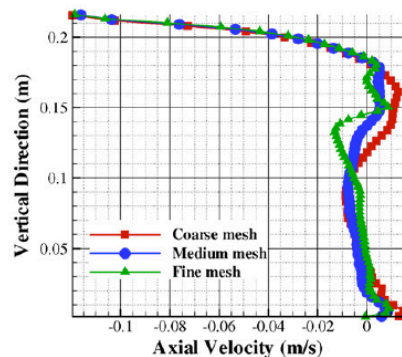
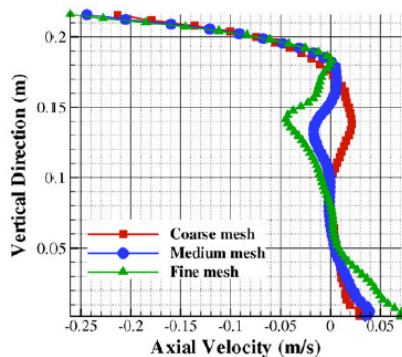
Mostly, the turbulence models are varied, the numerical method is rather poorly described. They run the solution on three meshes and do an extensive comparison. Not perfect, but much better than 95% of the literature!

the time averaged equations. If the primary interest is in the mean steady flow quantities, then these should be extracted from the unsteady solutions via long-time averaging, as it is the case in the

Acronym	Turbulence model	Grid	Re	Comments
SST-C-H	SST $k-\omega$	Coarse	High	Enhanced wall treatment used
SST-M-H	SST $k-\omega$	Medium	High	Enhanced wall treatment used
SST-F-H	SST $k-\omega$	Fine	High	Enhanced wall treatment used
RNG-C-H	RNG $k-\epsilon$	Coarse	High	Enhanced wall treatment used
RNG-M-H	RNG $k-\epsilon$	Medium	High	Enhanced wall treatment used
RNG-F-H	RNG $k-\epsilon$	Fine	High	Enhanced wall treatment used
SST-C-L	SST $k-\omega$	Coarse	Low	Low Re variants used
RNG-C-L	RNG $k-\epsilon$	Coarse	Low	Low Re effective viscosity used

ry condi-
at length
ie outlet,

as vortex sl



5.1. Grid convergence and error estimation

One of the critical issues in such unsteady flow simulations is to perform a grid convergence assessment and quantify the numerical uncertainty in relation with the solution of the modeled equations. The uncertainty assessment procedure recommended by Journal of Fluids Engineering (JFE) (Celik et al., 2008) is applied first. Sample results shown in Fig. 14 indicate that the local values of the apparent order vary widely from point to point leading to unreasonably large uncertainty on the computed velocities.

When we use the average value of the apparent order, p , the uncertainty predictions exhibit a reasonable distribution for SST

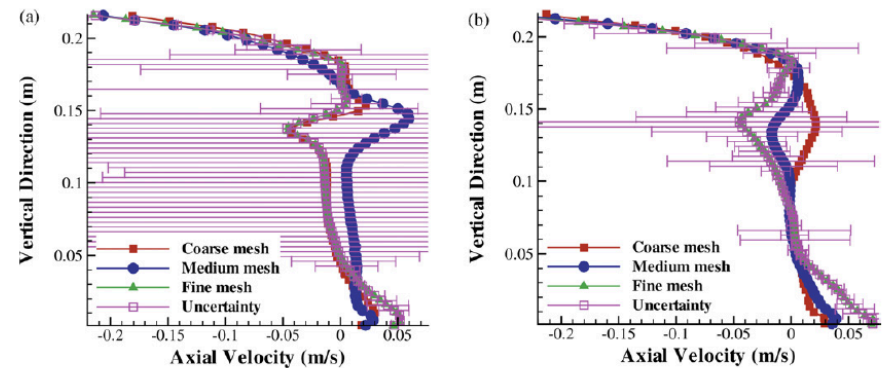


Fig. 14. Predicted uncertainties with JFE method at P2 using (a) SST $k-\omega$ model and (b) RNG $k-\epsilon$ model, using local values of the apparent order, p .

Grid convergence, uncertainty and accuracy is assessed. My only real complaint is that the numerical uncertainty is most likely to be a one-sided bias rather than a two-sided uncertainty as depicted here.

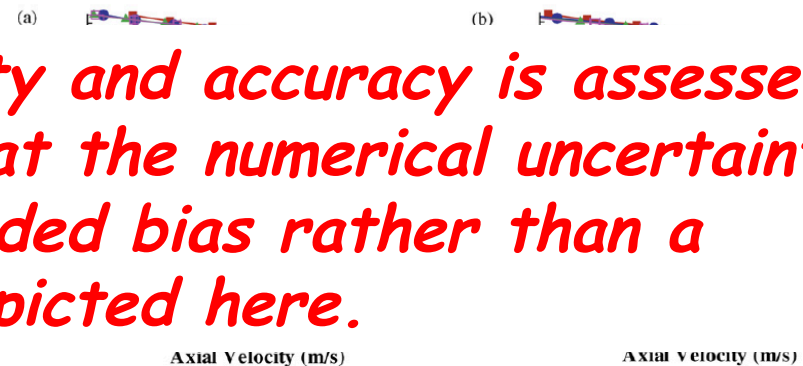


Fig. 15. Predicted uncertainties with JFE method and averaged p (order) at P2 using (a) SST $k-\omega$ model and (b) RNG $k-\epsilon$ model.

Table 5
Global convergence ratio, R_2 values at different locations.

	P1	P2	P3	P4	P5	P6
RNG $k-\epsilon$ model						
Axial velocity	1.86	1.12	1.03	1.09	1.28	1.12
Transverse velocity	1.45	1.01	1.07	1.01	1.04	1.18
Vertical velocity	3.06	1.23	1.27	1.16	1.20	1.04
SST $k-\omega$ model						
Axial velocity	1.04	1.17	0.99	0.77	1.01	1.13
Transverse velocity	2.24	0.97	1.13	0.89	0.92	1.81
Vertical velocity	1.48	0.36	0.95	0.83	1.12	1.20



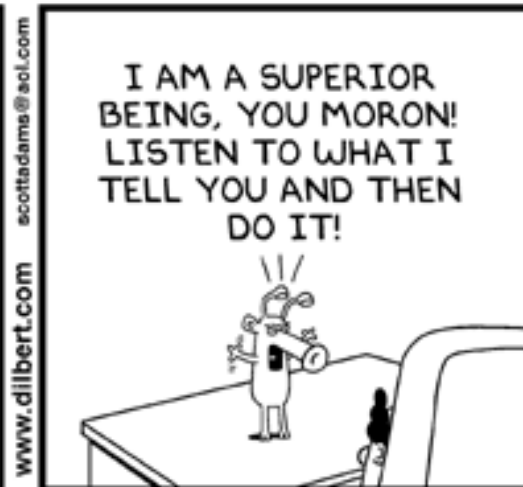
“A computer lets you make more mistakes faster than any invention in human history — with the possible exceptions of handguns and tequila.”

Mitch Ratliffe, Technology Review, April, 1992

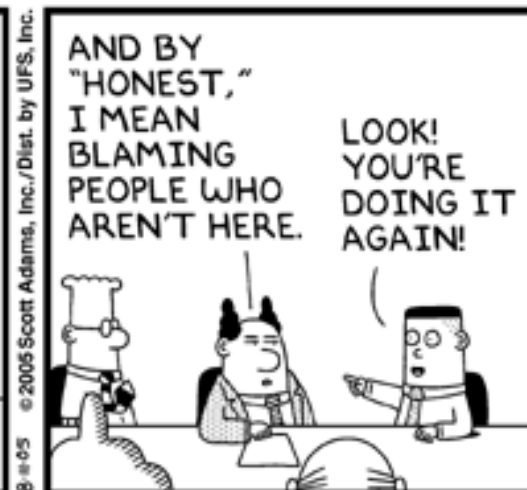




“Dilbert isn’t a comic strip, it’s a documentary” – Paul Dubois



© Scott Adams, Inc./Dist. by UFS, Inc.



© Scott Adams, Inc./Dist. by UFS, Inc.